





The ribosomal chaperone NACA recruits PHD2 to cotranslationally modify HIF- α

Daisheng Song¹ , Kai Peng¹ , Bradleigh E Palmer²  & Frank S Lee^{3*} 

Abstract

Prolyl hydroxylase domain protein 2 (PHD2)-catalyzed modification of hypoxia-inducible factor (HIF)- α is a key event in oxygen sensing. We previously showed that the zinc finger of PHD2 binds to a Pro-Xaa-Leu-Glu (PXLE) motif. Here, we show that the zinc finger binds to this motif in the ribosomal chaperone nascent polypeptide complex- α (NACA). This recruits PHD2 to the translation machinery to cotranslationally modify HIF- α . Importantly, this cotranslational modification is enhanced by a translational pause sequence in HIF- α . Mice with a knock-in *Naca* gene mutation that abolishes the PXLE motif display erythrocytosis, a reflection of HIF pathway dysregulation. In addition, human erythrocytosis-associated mutations in the zinc finger of PHD2 ablate interaction with NACA. Tibetans, who have adapted to the hypoxia of high altitude, harbor a PHD2 variant that we previously showed displays a defect in zinc finger binding to p23, a PXLE-containing HSP90 cochaperone. We show here that Tibetan PHD2 maintains interaction with NACA, thereby showing differential interactions with PXLE-containing proteins and providing an explanation for why Tibetans are not predisposed to erythrocytosis.

Keywords hypoxia-inducible factor; NACA; prolyl hydroxylase domain protein 2; Tibetan adaptation

Subject Categories Post-translational Modifications & Proteolysis; Translation & Protein Quality

DOI 10.15252/emboj.2022112059 | Received 7 July 2022 | Revised 23 August 2022 | Accepted 23 September 2022 | Published online 11 October 2022

The EMBO Journal (2022) 41: e112059

Introduction

A central event in the oxygen-sensing hypoxia-inducible factor (HIF) pathway is site-specific prolyl hydroxylation of HIF- α catalyzed by prolyl hydroxylase domain protein (PHD) (Kaelin & Ratcliffe, 2008; Semenza, 2012). This modification targets HIF- α for recognition by the von Hippel Lindau protein and subsequent degradation by the ubiquitin-proteasome pathway. Under hypoxic conditions, this oxygen-dependent modification is arrested, leading to HIF- α stabilization, its dimerization with HIF- β (also known as

ARNT), and the subsequent binding of the HIF- α :HIF- β heterodimer to hypoxia response elements that regulate hundreds of genes that facilitate adaptation to hypoxia. In mammals, there are two main HIF- α paralogues, HIF-1 α and HIF-2 α , which regulate overlapping as well as distinct genes. HIF-1 α is the principal paralogue that regulates genes encoding enzymes of glycolysis, thereby promoting a shift from oxidative phosphorylation to glycolysis. HIF-2 α (also known as EPAS1) regulates the *ERYTHROPOIETIN* gene, the product of which regulates red cell mass in an oxygen-sensitive manner. Loss of function human *HIF2A* mutations are associated with erythrocytosis (Lee & Percy, 2011; Lappin & Lee, 2019).

In mammals, there are three PHD paralogues, PHD1, PHD2, and PHD3 (also known as EGLN2, EGLN1, and EGLN3, respectively) (Bruick & McKnight, 2001; Epstein *et al.*, 2001; Ivan *et al.*, 2002). PHD2 is a key paralogue that is ancestrally related to the single PHD orthologues present in organisms such as *Caenorhabditis elegans* and the simplest metazoan, *Trichoplax adhaerens* (Loenarz *et al.*, 2011). PHD2 consists of two evolutionarily conserved domains, an N-terminal zinc finger (ZF) domain and a C-terminal prolyl hydroxylase domain. Human heterozygous loss of function mutations in the catalytic domain of PHD2 are associated with erythrocytosis, which is phenocopied by a mouse bearing a knock-in mutation of one of these erythrocytosis-associated *PHD2* mutations (Percy *et al.*, 2006; Arsenault *et al.*, 2013; Gardie *et al.*, 2014). The N-terminal domain binds to a Pro-Xaa-Leu-Glu motif present in proteins that include the HSP90 cochaperones p23 and FKBP38, as well as the two cytosolic HSP90 paralogues, HSP90 α and HSP90 β (Song *et al.*, 2013, 2014). HIF- α is a client of the HSP90 pathway, leading to a model in which the ZF of PHD2 promotes its recruitment to the HSP90 pathway to facilitate prolyl hydroxylation of HIF- α .

Importantly, human loss of function mutations have also been identified that affect PHD2 ZF function. Some, including Y41C, C42R, and K55N, are in the ZF itself and are associated with erythrocytosis (Sinnema *et al.*, 2018; Song *et al.*, 2019). A mouse bearing knock-in mutations that ablate ZF integrity displays erythrocytosis (Arsenault *et al.*, 2016). Human erythrocytosis-associated mutations such as C42R abolish interaction with multiple PXLE-containing proteins, including p23 and FKBP38 (Sinnema *et al.*, 2018), and therefore do not identify the actual PHD2 ligand that is critical for normal erythropoiesis. A distinct pair of mutations that affect ZF function

Department of Pathology and Laboratory Medicine, Perelman School of Medicine, University of Pennsylvania, Philadelphia, PA, USA

*Corresponding author. Tel: +1 215 898 4701; E-mail: franklee@penmedicine.upenn.edu

[†]Present address: Chime Biologics, Wuhan, China

[‡]Present address: Department of Biology, Johns Hopkins University, Baltimore, MD, USA

has been reported in Tibetans, who have adapted to the chronic hypoxia of high altitude. They harbor two tightly linked mutations, D4E/C127S, that flank the ZF (Xiang *et al*, 2013; Lorenzo *et al*, 2014). This combination selectively impairs interaction with p23 but not with other HSP90 cochaperones such as FKBP38 (Song *et al*, 2014). A mouse model with a knock-in Tibetan *Phd2* mutation (D4E/C127S) displays augmented hypoxic ventilatory responses, which is phenocopied by a knock-in p23 mutation (L159A/E160A) that ablates the PXLE motif in p23, consistent with the notion that the impaired PHD2:p23 interaction is critical for the respiratory phenotype of Tibetan adaptation (Song *et al*, 2020). Tibetan *Phd2* mice display normal hematocrit and hemoglobin levels (Song *et al*, 2020).

In the present report, we examined hemoglobin levels and red blood cell counts in mice with knock-in PXLE > PXAA mutations in ligands of the PHD2 ZF, including p23, Fkbp38, Hsp90 α , Hsp90 β , and a more recently identified ligand, the ribosomal chaperone nascent polypeptide-associated complex- α (NACA). Interestingly, we observe that a PXLE > PXAA mutation in Naca, but not in the proteins of the HSP90 pathway, results in erythrocytosis, thereby identifying NACA as being a critical component of the pathway by which PHD2 controls red cell mass. NACA is a ribosomal chaperone that forms a heterodimer with NAC- β (NACB) and binds to the ribosome in the vicinity of the ribosomal exit tunnel (Wiedmann *et al*, 1994; Deuerling *et al*, 2019; Gamerdinger *et al*, 2019; Jomaa *et al*, 2022). It directs cytosolic polypeptides to their correct cellular locale. We furthermore provide evidence that an evolutionarily conserved translational pause site in HIF-2 α facilitates PHD2-catalyzed, cotranslational prolyl hydroxylation of HIF-2 α . Finally, we show that the Tibetan D4E/C127S PHD2 mutant, in contrast to erythrocytosis-associated PHD2 ZF mutations, maintains interaction with NACA and the capacity to cotranslationally modify HIF-2 α , thereby providing an explanation of why individuals with the Tibetan PHD2 mutations are not predisposed to erythrocytosis.

Results

The PXLE motif of NACA is essential for normal control of red cell mass

Prolyl hydroxylase domain protein 2 binds to the PXLE motif in the HSP90 cochaperones p23 and FKBP38, as well as HSP90 itself (which consists of two paralogues, HSP90 α and HSP90 β) (Song *et al*, 2013, 2014). In order to assess which of these PHD2 binding partners might be important for the control of red cell mass in mice, one could in principle simply delete that partner. However, homozygous knockouts of the candidate partners cannot be employed because they lead to embryonic lethality (Hsp90 β), male sterility (Hsp90 α), perinatal lethality (p23), or neural tube defects (Fkbp38) (Voss *et al*, 2000; Bulgakov *et al*, 2004; Grad *et al*, 2006, 2010). Moreover, the interpretation of such knockouts would undoubtedly be complicated by the loss of broad, HIF-independent functions of these ubiquitously expressed proteins. We, therefore, chose to generate knock-in mice in which we selectively ablated their interactions with Phd2 by introducing PXLE > PXAA substitutions. In all of these candidate proteins, available data suggest that the PXLE motif resides in an unstructured, exposed portion of the protein,

indicating that such mutations would be unlikely to disrupt the overall fold of the protein (Ali *et al*, 2006).

We previously showed that PXLE > PXAA mutations in p23 and FKBP38 abolish interaction with PHD2 and described the generation of p23^{AA} (L159A/E160A) and *Fkbp38*^{AA} (L45A/E46A) knock-in mouse lines (Song *et al*, 2020). Protein levels of Fkbp38 were not appreciably affected in kidneys, livers, hearts, and lungs of *Fkbp38*^{AA/AA} mice (Appendix Fig S1A). Protein levels of p23 were not significantly affected in kidneys or livers of p23^{AA/AA} mice and were somewhat decreased in the heart and lungs (Appendix Fig S1B). For both mouse lines, Phd2 protein levels were not appreciably affected in the tissues examined. We pursued an analogous approach with Hsp90. *In vitro*, we find that a PXLE > PXAA (L711A/E712A) mutation in HSP90 β abolishes binding to PHD2 (Fig EV1A, top panel). We employed Crispr to generate PXLE > PXAA mutations in the two Hsp90 paralogues, Hsp90 α and Hsp90 β in mice (Fig EV1B and C) and generated *Hsp90 α* ^{AA/AA} (L720A/E721A), *Hsp90 β* ^{AA/AA} (L711A/E712A), and *Hsp90 α* ^{AA/AA}; *Hsp90 β* ^{AA/AA} mice. Hsp90 and Phd2 protein levels were not appreciably affected in kidneys, livers, hearts, and lungs of *Hsp90 α* ^{AA/AA}; *Hsp90 β* ^{AA/AA} mice (Appendix Fig S1C). We measured hemoglobin, hematocrit, and red blood cell counts in p23^{AA/AA}, *Fkbp38*^{AA/AA}, *Hsp90 α* ^{AA/AA}, and *Hsp90 β* ^{AA/AA} mice. We did not observe any differences in these indices between any of these knock-in mice and wild-type control mice (Fig EV2A–D). A similar result was obtained with combinations of these knock-ins, including *Hsp90 α* ^{AA/AA}; *Hsp90 β* ^{AA/AA} mice and *Fkbp38*^{AA/AA}; *Hsp90 α* ^{AA/AA}; *Hsp90 β* ^{AA/AA} mice (Fig EV2E and F).

In a previous Stable Isotope Labeling by Amino Acids in Cell Culture (SILAC) study, we identified p23, FKBP38, HSP90 α , and HSP90 β by mass spectrometry in PHD2 immunoprecipitates (Song *et al*, 2013, 2014). We also observed enrichment of NACA in these immunoprecipitates (heavy isotope to light isotope ratio = 4.3), but did not pursue studies on NACA at that time. Inspection of the NACA sequence reveals the presence of a PXLE motif, similar to that found in p23, FKBP38, HSP90 α , and HSP90 β (Fig 1A). As in the other proteins, the Pro of the PXLE motif in NACA is preceded by a hydrophobic residue, and acidic residues are present N-terminal to this hydrophobic residue. This motif is highly conserved among vertebrates (Fig 1B). We coexpressed PHD2 and NACA in HEK293FT cells, immunoprecipitated the latter, and confirmed binding between the two (Fig 1C). Mutation of the PXLE motif to PXAA abolishes this interaction, consistent with the ZF of PHD2 binding to this PXLE motif in NACA.

Nascent polypeptide-associated complex- α binds to NAC- β (NACB) to form a heterodimeric NAC complex (Wiedmann *et al*, 1994). NAC, in turn, resides at the exit site of the ribosomal exit tunnel, and it is an essential factor that is among the first proteins that nascent polypeptides encounter as they emerge from the ribosome exit tunnel. NAC directs cytosolic polypeptides to the cytoplasm, and it competes with signal recognition particle (SRP), which directs nascent polypeptides with signal sequences to the endoplasmic reticulum (Wiedmann *et al*, 1994; Gamerdinger *et al*, 2015; Jomaa *et al*, 2022). This raises the possibility that NACA might recruit PHD2 to the ribosome to facilitate prolyl hydroxylation of the nascent HIF- α polypeptide.

Homozygous knockout of Naca in mice is embryonic lethal, consistent with its essential role as a chaperone for protein sorting at

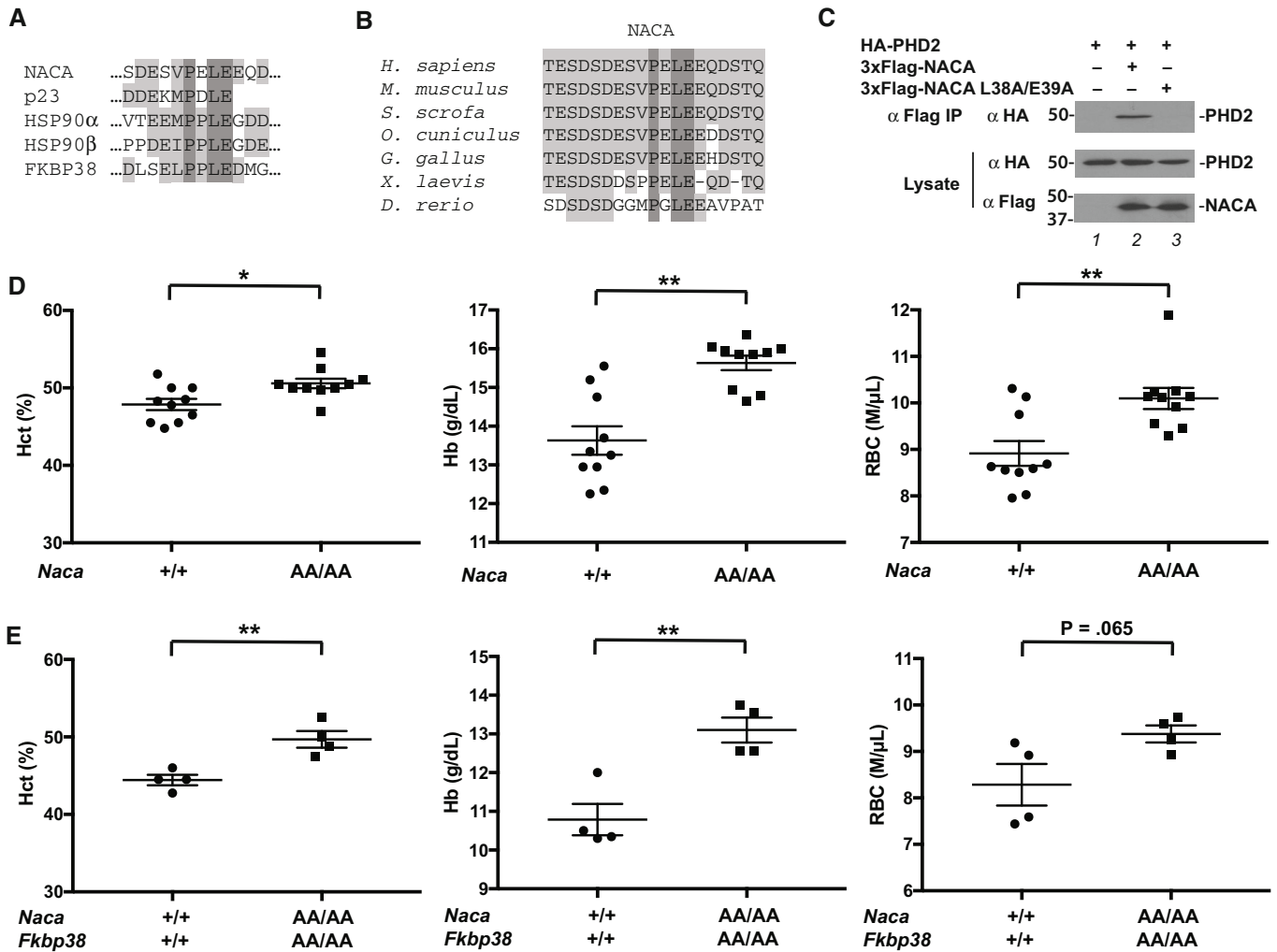


Figure 1. PHD2 binds to a PXLE motif in NACA, and *Naca*^{AA/AA} mice display erythrocytosis.

A Comparison of PXLE motifs in human NACA, p23, HSP90 α , HSP90 β , and FKBP38. Dark shading highlights the P, L, and E of the PXLE motif. Light shading highlights conserved residues.

B Comparison of NACA sequence from human (residues 27–45) with those from mouse, pig, rabbit, chicken, frog, and zebrafish. Dark shading highlights the P, L, and E of the PXLE motif. Light shading highlights residues identical to those in human NACA.

C HEK293 FT cells were transfected with expression plasmids for the indicated proteins. The cells were lysed and subjected to immunoprecipitation with anti-Flag antibodies, and then the immunoprecipitates and aliquots of lysate were examined by western blotting as indicated.

D, E Hct, Hb, and RBC counts were measured in (D) *Naca*^{AA/AA} and (E) *Naca*^{AA/AA}; *Fkbp38*^{AA/AA} mice and compared to wild-type controls. In (D), $n = 10$ with five males and five females in each group. In (E), $n = 4$ with four males in each group. Biological replicates, with mean \pm SEM are shown. * $P < 0.05$, ** $P < 0.01$, by unpaired two-tailed t-test.

the ribosome (Hekmatnejad *et al*, 2014). We, therefore, used Crispr to generate mice with the PXLE > PXAA mutation (L38A/E39A) that abolishes interaction with PHD2 (Fig EV1D). Structural and functional studies suggest that the PXLE motif resides in an unstructured, flexible region of the protein away from the ribosome-binding NAC domain of this protein (Liu *et al*, 2010; Martin *et al*, 2018; Deuerling *et al*, 2019; Gamerdinger *et al*, 2019), indicating that this mutation is unlikely to affect the overall fold of this protein. Mice homozygous for the mutation (*Naca*^{AA/AA}) were outwardly normal and fertile. *Naca* and *Phd2* protein levels were not appreciably affected in kidneys, livers, hearts, and lungs of *Naca*^{AA/AA} mice (Appendix Fig S1D). Importantly, we found that *Naca*^{AA/AA} mice

have elevated hematocrit, hemoglobin levels, and red cell counts compared to controls (Fig 1D). Serum Epo levels were not elevated in these mice (Fig EV1E). It might be noted that humans and mice with erythrocytosis due to *PHD2* mutations often display normal serum EPO levels; in this context, the EPO levels are regarded as inappropriately normal (Gardie *et al*, 2014).

We found that the *Naca*^{AA/AA} mutation in an *Fkbp38*^{AA/AA} background also results in erythrocytosis (Fig 1E). The *Naca*^{AA/AA}; *Fkbp38*^{AA/AA} mice were generated by appropriate intercrosses. In the case of *p23*, such an approach was not feasible because the *Naca* and *p23* genes are adjacent to one another on the same chromosome (Fig EV3A). We, therefore, used Crispr and treated *p23*^{AA/+} fertilized

oocytes with a mixture of the Naca gRNA, Cas9 mRNA, and the 200 nucleotides single-stranded oligodeoxynucleotide donor previously employed to successfully generate the *Naca*^{AA} allele. While we did not obtain any *Naca*^{AA/AA}; *p23*^{AA/+} mice, we did obtain a mouse with a *Naca*^{Δ/Δ}; *p23*^{AA/+} genotype, where Δ indicates a 6 bp in-frame deletion that removes the Leu-Glu dipeptide from the PXLE motif (Fig EV3B). *In vitro* coimmunoprecipitation experiments reveal that this two-amino acid deletion abolishes interaction between NACA and PHD2 (Fig EV3C). We generated *Naca*^{Δ/Δ}; *p23*^{AA/AA} mice from crosses of *Naca*^{Δ/+}; *p23*^{AA/+} and *Naca*^{Δ/+}; *p23*^{AA/+} mice. We observed that mice with a *Naca*^{Δ/Δ} mutation in a *p23*^{AA/AA} background display increased Hct (Fig EV3D). Taken together with other results, the data identify the Naca PXLE motif as being critical for maintaining normal red cell mass.

We analyzed transcripts for the Hif target genes *Epo*, *Glut1*, *Pgk1*, *Ndr1*, *Edn1*, and *Vegfa* in the kidneys from wild-type and *Naca*^{AA/AA} mice by real-time PCR. A trend toward increased *Epo* mRNA was seen in kidneys from *Naca*^{AA/AA} mice as compared to controls (Fig EV4A); however, it was not statistically significant ($P = 0.24$). No differences were seen in levels of the other transcripts (Fig EV4B–F). *Epo* transcript was not detectable in livers from either wild-type or *Naca*^{AA/AA} mice.

Evidence that NACA recruits PHD2 to the ribosome

The known biological function of NACA in chaperoning nascent polypeptides raises the possibility that NACA might recruit PHD2 to the ribosome to facilitate prolyl hydroxylation of HIF- α . We performed *in vitro* translation reactions to test this. We employed reticulocyte lysates, which have been extensively used to characterize mammalian protein translation (Jagus & Beckler, 2003). These lysates contain endogenous PHD2, which might confound experiments designed to directly measure prolyl hydroxylation (Jaakkola et al, 2001; Ivan et al, 2002). We, therefore, employed a previously described assay (Arsenault et al, 2016) in which we employed a fusion protein consisting of the ZF of PHD2 and the *E. coli* biotin ligase BirA (Fig 2A, second construct from top), and examined biotinylation of polypeptides containing an embedded biotin acceptor peptide (BAP) as a surrogate marker for prolyl hydroxylation (Fig 2B). We prepared the BirA fusion protein as well as a mutant fusion protein which contains a C36S/C42S mutation (Song et al, 2013) that disables the ZF (Fig 2A, third construct from top, and Fig 2C). We then examined the capacity of the fusion proteins to biotinylate an *in vitro* translated HIF-2 α polypeptide in which the primary site of prolyl hydroxylation in HIF-2 α has been replaced by the BAP motif (Fig 2D, construct 1). Far western blotting using streptavidin then allows assessment of the degree of HIF-2 α biotinylation. As shown in Fig 2E (top panel), the wild-type PHD2 ZF fused to BirA readily biotinylates HIF-2 α BAP, and this biotinylation is diminished by the inactivating C36S/C42S ZF mutation, as seen previously (Arsenault et al, 2016).

We next examined two BAP motif-containing HIF-2 α fragments. One consists of the N-terminal half of HIF-2 α and contains the basic helix–loop–helix (bHLH), Per-Arnt-Sim (PAS), and N-terminal oxygen-dependent degradation (NODD) domains (Fig 2D, construct 2). The other consists of sequences flanking the primary site of prolyl hydroxylation (Fig 2D, construct 3). As shown in Fig 2F (top panel, lanes 2 and 4), the latter, but not the former, is efficiently

biotinylated by PHD2 ZF-BirA, and moreover, this biotinylation is sensitive to the ZF mutation. Because sequences N-terminal to the BAP motif are shared between the two constructs, this suggests that sequences C-terminal to the BAP motif might confer sensitivity to ZF mutation.

If NACA recruits the PHD2 ZF to the ribosome, we would predict that translational stalling of BAP-containing polypeptides should enhance the biotinylation catalyzed by the PHD2 ZF BirA fusion, since stalling should increase the time the nascent polypeptide is in the vicinity of the BirA fusion protein. To test this, we generated a construct in which a hemagglutinin (HA)-tagged green fluorescent protein (GFP) was fused to the BAP sequence, followed by an optimized translational arrest peptide (TAP) of XBP1u (Yanagitani et al, 2011; Shanmuganathan et al, 2019) (Fig 2G, construct 5). The XBP1u TAP adopts a distinctive conformation in the ribosomal peptide tunnel that arrests translation (Shanmuganathan et al, 2019), the biological function of which is to allow the association of an upstream XBP1u polypeptide sequence with the endoplasmic reticulum. When *in vitro* translated, we observe that this GFP-HA-BAP-TAP protein is readily biotinylated by PHD2 ZF-BirA in a manner sensitive to ZF integrity (Fig 2H, top panel). Moreover, the biotinylation is diminished by a TAP mutation (V254P/A255S/W256A) that abrogates its capacity to arrest translation (Shanmuganathan et al, 2019) (Fig 2G, construct 6, and Fig 2I, top panel). This mutant substrate is insensitive to mutations that ablate the PHD2 ZF (Fig 2J). These observations support a model in which NACA recruits the ZF of PHD2 to the ribosome.

Translational pausing of HIF-2 α potentiates its prolyl hydroxylation by PHD2

The results just described lead us to consider the possibility that a sequence in HIF-2 α might itself cause translational pausing and thereby promote NACA-mediated, PHD2-catalyzed hydroxylation of HIF-2 α . We reasoned that such a sequence would be conserved through evolution. We examined the conservation of residues in HIF-2 α across vertebrate species (HIF-2 α is not present in invertebrates). In addition to the well-characterized bHLH domain, PAS domain, NODD, C-terminal oxygen-dependent degradation domain, and C-terminal activation domain, we noted a highly conserved, 34 amino acid sequence (residues 620–653) that resides about 100 amino acids C-terminal to the primary site of prolyl hydroxylation (this region is colored in red in Fig 3A). It contains a motif, WPPDPP, that contains multiple copies of a Pro-(Pro/Gly/Asp) dipeptide motif that is enriched in polypeptide sequences in collided ribosome pairs (disomes) which result from translational pausing (Han et al, 2020). More notably, it contains a Pro-Pro-Asp tripeptide motif (orange box in Fig 3A) that is among the most highly enriched tripeptide sequences occupying the exit-peptidyl-aminoacyl (E-P-A) sites of the downstream ribosome of disomes in HEK293 cells (Han et al, 2020).

To test the possibility that this sequence might mediate translational pausing and thereby facilitate the activity of the PHD2 ZF-BirA fusion protein (and by inference, the hydroxylase activity of PHD2), we substituted the TAP sequence of GFP-HA-BAP-TAP with the HIF-2 α sequence noted above (Fig 3B, construct 7). As shown in Fig 3C (top panel, lanes 4 and 5, top bands), the resulting construct

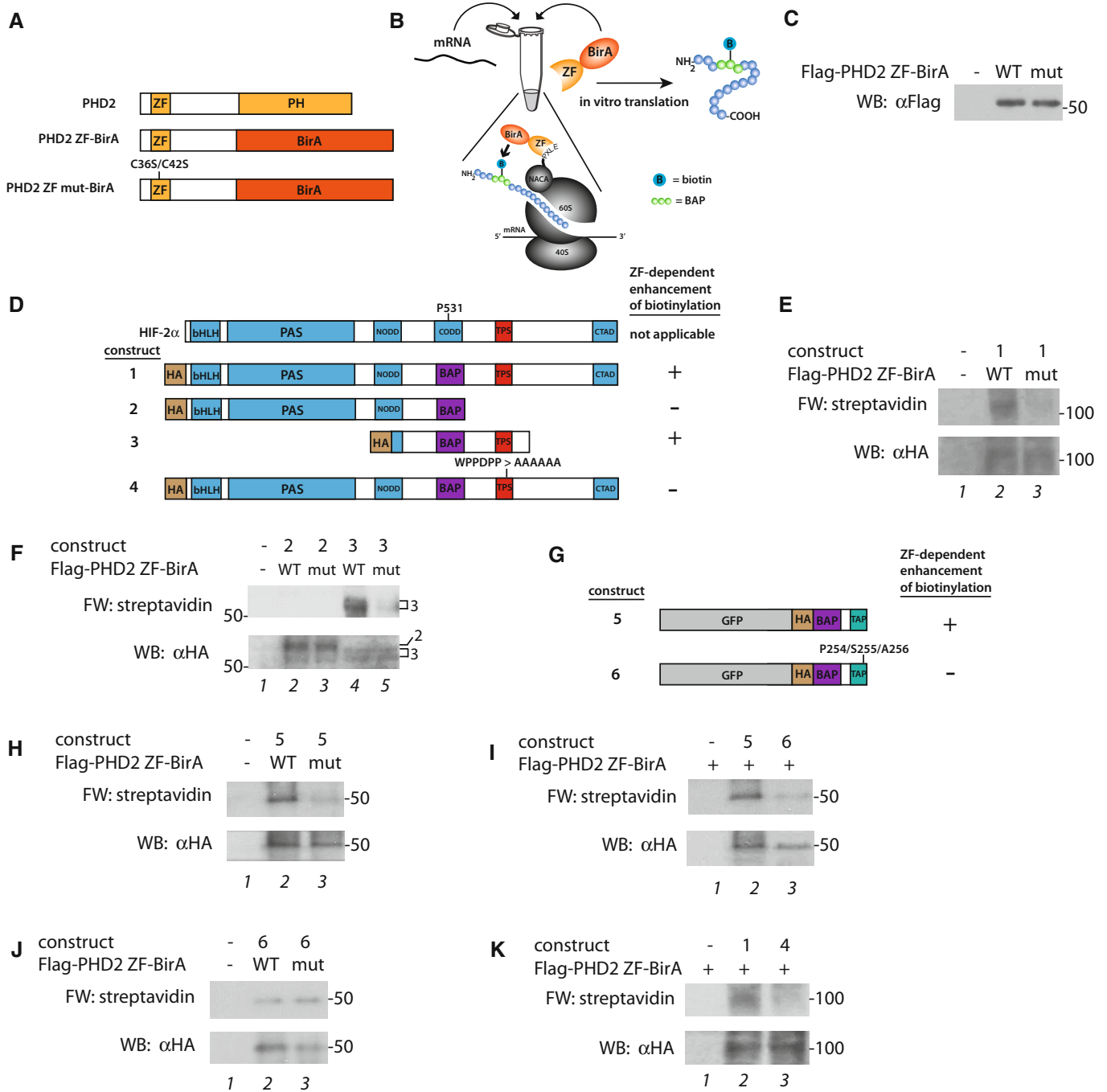


Figure 2. PHD2 zinc finger is recruited to the ribosome by its zinc finger.

A Diagram of PHD2 and constructs employed for *in vitro* translation studies. ZF, zinc finger; PH, prolyl hydroxylase domain. Mutations are as indicated.
B *In vitro* translation/biotinylation reaction. BAP, biotin acceptor peptide. 60S and 40S subunits of ribosome are as indicated.
C Proteins were prepared by *in vitro* translation using reticulocyte lysates and analyzed by αFlag western blotting.
D Diagram of HIF-2α and constructs employed for *in vitro* translation studies. HA, hemagglutinin; bHLH, basic helix-loop-helix; PAS, Per-Arnt-Sim domain; NODD, N-terminal oxygen-dependent degradation domain; CDD, C-terminal oxygen-dependent degradation domain; CTAD, C-terminal activation domain; BAP, biotin acceptor peptide; TPS, translation pause sequence. P531 is the primary site of prolyl hydroxylation in HIF-2α. The capacity of the PHD2 zinc finger to enhance biotinylation of the indicated constructs is summarized to the right.
E–K *In vitro* translation/biotinylation reactions using reticulocyte lysates and the indicated constructs (E, F, H–K). Streptavidin far western (FW) assesses biotinylation. Anti-HA western blot (WB) measures translated protein. (G) Diagram of constructs employed for *in vitro* translation studies. GFP, green fluorescent protein; TAP, translation arrest peptide from XBP1u. The capacity of the PHD2 zinc finger to enhance biotinylation of the indicated constructs is summarized to the right.

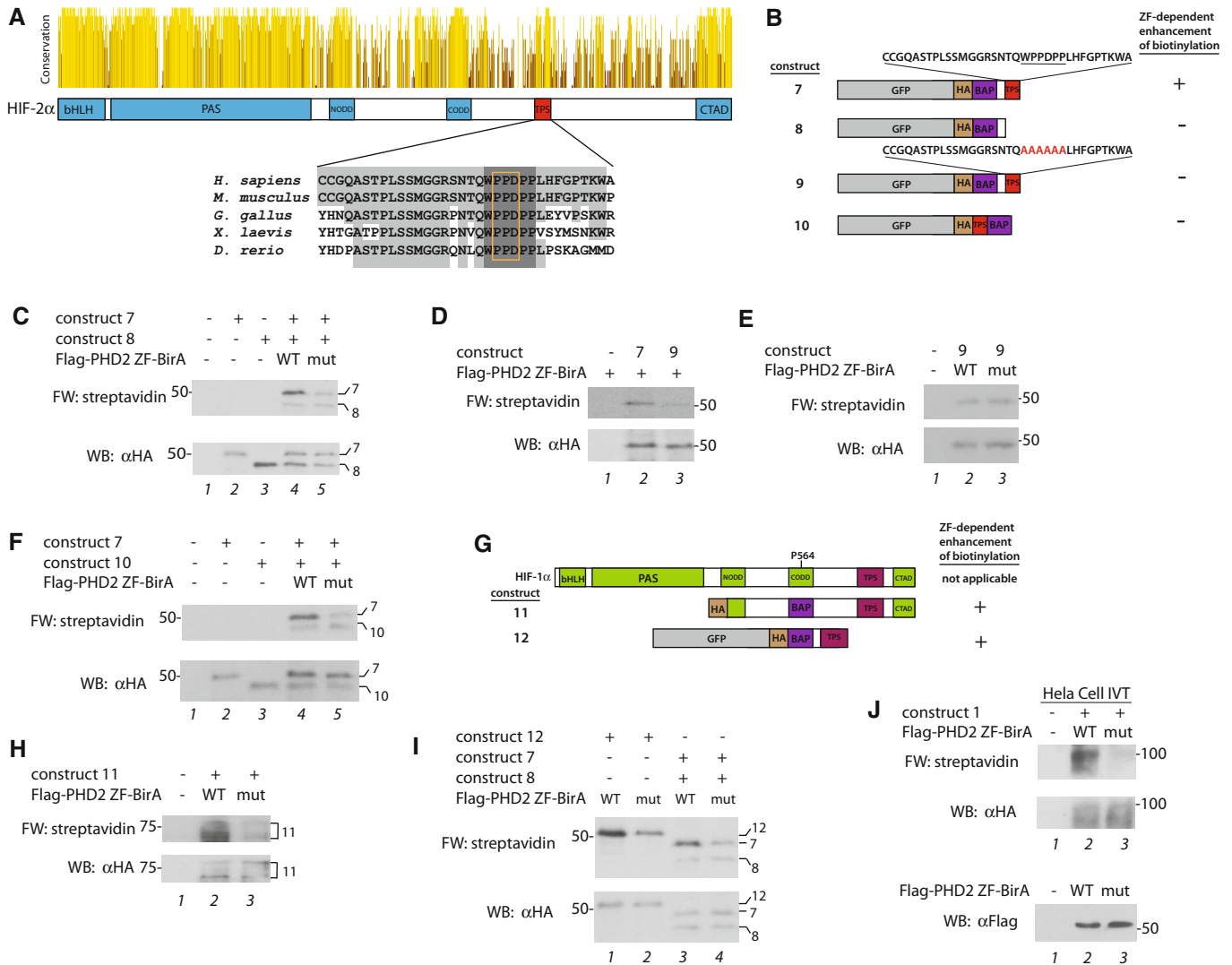


Figure 3. HIF-2α contains a conserved translational pause sequence.

A Sequence conservation of HIF-2α across 203 vertebrate species. Sequences were aligned using MUSCLE (Edgar, 2004) and visualized using Jalview (Waterhouse et al, 2009). Bottom, sequence of proposed TPS in HIF-2α across species. Light shading = residues identical to human HIF-2α. Dark shading = WPPDPP motif. Orange box = PPD motif.

B-I (B, C) Diagram of constructs employed for *in vitro* translation studies. In construct 7, underlining indicates sequence that is mutated in construct 9. In (G), P564 indicates the primary site of prolyl hydroxylation in HIF-1α, and TPS is the proposed translational pause sequence. The capacity of the PHD2 zinc finger to enhance biotinylation of the indicated constructs is summarized to the right. (C-F, H, I) *In vitro* translation/biotinylation reactions using reticulocyte lysates and the indicated constructs. Streptavidin far western (FW) assesses biotinylation. Anti-HA western blot (WB) measures translated protein.

J *In vitro* translation (IVT)/biotinylation reactions using HeLa cell lysates and the indicated constructs. Streptavidin far western (FW) assesses biotinylation. Anti-HA western blot (WB) measures translated protein. Bottom, the indicated proteins were prepared by *in vitro* translation using HeLa cell lysates and analyzed by αFlag western blotting.

is biotinylated by PHD2 ZF BirA in a manner sensitive to ZF integrity. As an internal control, construct 8 (Fig 3B), which lacks the HIF-2α sequence, was translated in the same reaction and we find that biotinylation of this construct is not enhanced by the ZF (Fig 3C, top panel, lanes 4 and 5, bottom bands). Mutation of the WPPDPP motif to AAAAAA reduces biotinylation (Fig 3B, construct 9, and Fig 3D, top panel). This mutant substrate is insensitive to mutations that ablate the integrity of the PHD2 ZF (Fig 3E). Mutation of this WPPDPP motif in the context of full-length HIF-2α BAP

also impairs biotinylation (Fig 2D, construct 4, and Fig 2K, top panel). As a further test of specificity, we compared the behavior of this HIF-2α sequence with that immediately downstream of the primary site of prolyl hydroxylation (Fig EV5A, construct 13). Again, ZF-dependent enhancement of biotinylation is seen with the former (Fig EV5B, top panel, lanes 4 and 5, top bands) but not the latter (top panel, lanes 4 and 5, bottom bands). On the basis of these findings, we designate the 34 amino acid sequence in HIF-2α a translational pause sequence (TPS).

A critical prediction of our model is directionality—i.e., the enhancement due to ZF recruitment should only be seen when the pause sequence is C-terminal to the site of posttranslational modification. We tested this by placing the pause sequence N-terminal to the BAP sequence in a GFP-HA-HIF-2 α -TPS-BAP construct (Fig 3B, construct 10). As shown in Fig 3F, under conditions in which enhancement of biotinylation is readily seen in GFP-HA-BAP-HIF-2 α TPS (construct 7; top panel, lanes 4 and 5, top bands), it is abolished when the pause sequence placed before the BAP motif (top panel, lanes 4 and 5, bottom bands). Thus, the pause sequence acts in cis and depends on its positioning with respect to the site of cotranslational modification.

Examination of GFP-HA-BAP fused to a shorter 22 amino acid HIF-2 α sequence (residues 624–645) does not show enhancement of biotinylation in a ZF-dependent manner (Fig EV5A, construct 14, and Fig EV5C, top panel). Additional N- and C-terminal truncations also fail to reveal enhancement of biotinylation (Fig EV5A, constructs 15 and 16, and Fig EV5D, top panel).

The experiments just described examined HIF-2 α . Examination of a fragment of HIF-1 α that contains its C-terminal half and that lacks its bHLH and PAS domains (Fig 3G, construct 11) is also biotinylated in a manner sensitive to the ZF mutation (Fig 3H, top panel). Examination of HIF-1 α sequences across species reveals a conserved 58 amino acid sequence (residues 702–759) within this C-terminal half of HIF-1 α (Fig EV5E). Fusion of this HIF-1 α sequence to the GFP-HA-BAP construct (Fig 3G, construct 12) results in enhancement of biotinylation in a ZF-dependent manner (Fig 3I, top panel, lanes 1 and 2), similar to that seen with GFP-HA-BAP-HIF-2 α TPS (top panel, lanes 3 and 4, top bands), and dissimilar to the behavior of the GFP-HA-BAP negative control (top panel, lanes 3 and 4, bottom bands). This HIF-1 α sequence lacks the WPPDPP motif found in the TPS of HIF-2 α . Additional experiments will be required to identify specific determinants in the HIF-1 α sequence that promote translational pausing. Taken together, these studies suggest that translation pausing promotes prolyl hydroxylation of both HIF-1 α and HIF-2 α .

The *in vitro* translation experiments just described employed reticulocyte lysates. We also examined the full-length HIF-2 α BAP construct (Fig 2D, construct 1) using HeLa cell extracts. We prepared PHD2 ZF-BirA fusion proteins using these extracts, and we find that the wild-type version induces biotinylation of the HA-HIF-2 α BAP construct that is substantially diminished by the C32S/C36S ZF mutation (Fig 3J, top panel), similar to what is observed with this construct using reticulocyte lysates (Fig 2E).

Translational pausing would be predicted to lead to increased occupancy of the mRNA by ribosomes at the site of pausing. Ribosome profiling provides information on the distribution of ribosomes on mRNA. We inspected published ribosome profiling datasets, and we identified studies (Werner *et al*, 2015; Gameiro & Struhl, 2018; Chen *et al*, 2020) in which there is a prominent ribosomal footprint in the area of the predicted pause site on the *HIF2A* mRNA (Fig 4A). For comparison, a similar footprint is seen in these same studies at the known pause site of the *XBP1u* mRNA (Fig 4B). Importantly, the *HIF2A* ribosome footprint is centered on the Pro-Pro-Asp motif of the predicted *HIF2A* pause sequence, just as the *XBP1u* footprint is centered on the Leu-Met-Asn motif of the known *XBP1u* pause sequence. The Leu-Met-Asn motif of *XBP1u* occupies the E-P-A sites of the stalled ribosome (Shanmuganathan

et al, 2019), suggesting the Pro-Pro-Asp motif of HIF-2 α might do the same.

Translational pausing can lead to disomes resulting from ribosome collisions (Han *et al*, 2020; Meydan & Guydosh, 2021). Such disomes would not be readily apparent in conventional ribosomal profiling studies, which typically size select for monosomes (McGlincy & Ingolia, 2017). We examined whether disomes could be detected on the *HIF2A* mRNA. Our general approach was to lyse tissue, perform RNase I digestions, isolate RNA, and then reverse transcribe the *Hif2a* mRNA using a primer (RT-mHif2 3') that is complementary to the predicted disome linked to an adapter sequence (Fig 4A and Appendix Fig S2A) (Li *et al*, 2019). Using an appropriate *Hif2a* specific 5' real-time PCR primer (mHif2 disome 5') and a 3' real-time PCR primer (M13 reverse) that hybridizes to the adapter sequence, this then generates amplicons of sufficient size for detection by real-time PCR. This, in turn, allows assessment for the presence or absence of disomes. We performed measurements on RNA in which the RNase I digestion was omitted to provide a reference point for calculating ΔC_T values ($\Delta C_T = C_{T-RNase} - C_{T+RNase}$). We also performed measurements using a negative control primer pair hybridizing well upstream of the predicted disome site (Appendix Fig S2A), as well as parallel experiments using primers for the known *Xbp1u* pause site (Fig 4B and Appendix Fig S2B).

Following lysis of mouse kidney, RNase I digestion, and isolation of RNA, we performed a single reverse transcription using the RT-mHif2 3' primer targeting the predicted *Hif2a* disome site, and we find that real-time PCR using primers to detect the predicted *Hif2a* disome lead to a significantly higher number of amplicons than control primers hybridizing well upstream of the predicted disome site (Fig 4C). In a control experiment with an analogous primer set, we observe the same result when testing for disomes at the known *Xbp1u* pause site (Fig 4D). In additional experiments, we performed two separate reverse transcription reactions—one targeting the predicted *Hif2a* disome site as before, the other targeting the control upstream site. Again, real-time PCR reveals higher amplicon counts for the predicted *Hif2a* disome than the control upstream site (Fig 4E), and the same result is seen in an experiment examining *Xbp1u* disomes at its known pause site (Fig 4F). These results provide evidence for the presence of disomes on the *Hif2a* mRNA at the predicted pause site.

Erythrocytosis-associated PHD2 zinc finger mutations impair binding to NACA

A subset of erythrocytosis-associated mutations in the *PHD2* gene is found in its ZF. We previously reported that these mutations, which include Y41C, C42R, and K55N, all impair the interaction between the PHD2 ZF and p23 (Sinnema *et al*, 2018; Song *et al*, 2019). In light of the erythrocytosis observed in *Naca*^{AA/AA} mice (Fig 1D), we extended these studies to NACA. We first coexpressed NACA and the PHD2 mutants in HEK293FT cells and performed coimmunoprecipitation experiments. In Fig 5A (top panel), we show that the three ZF mutations impair the interaction between the ZF and NACA. We next performed *in vitro* biotinylation assays. We fused all three ZFs to BirA, prepared recombinant versions of each by *in vitro* translation, and then tested them using the *in vitro* biotinylation assay. Consistent with previous results (Sinnema *et al*, 2018),

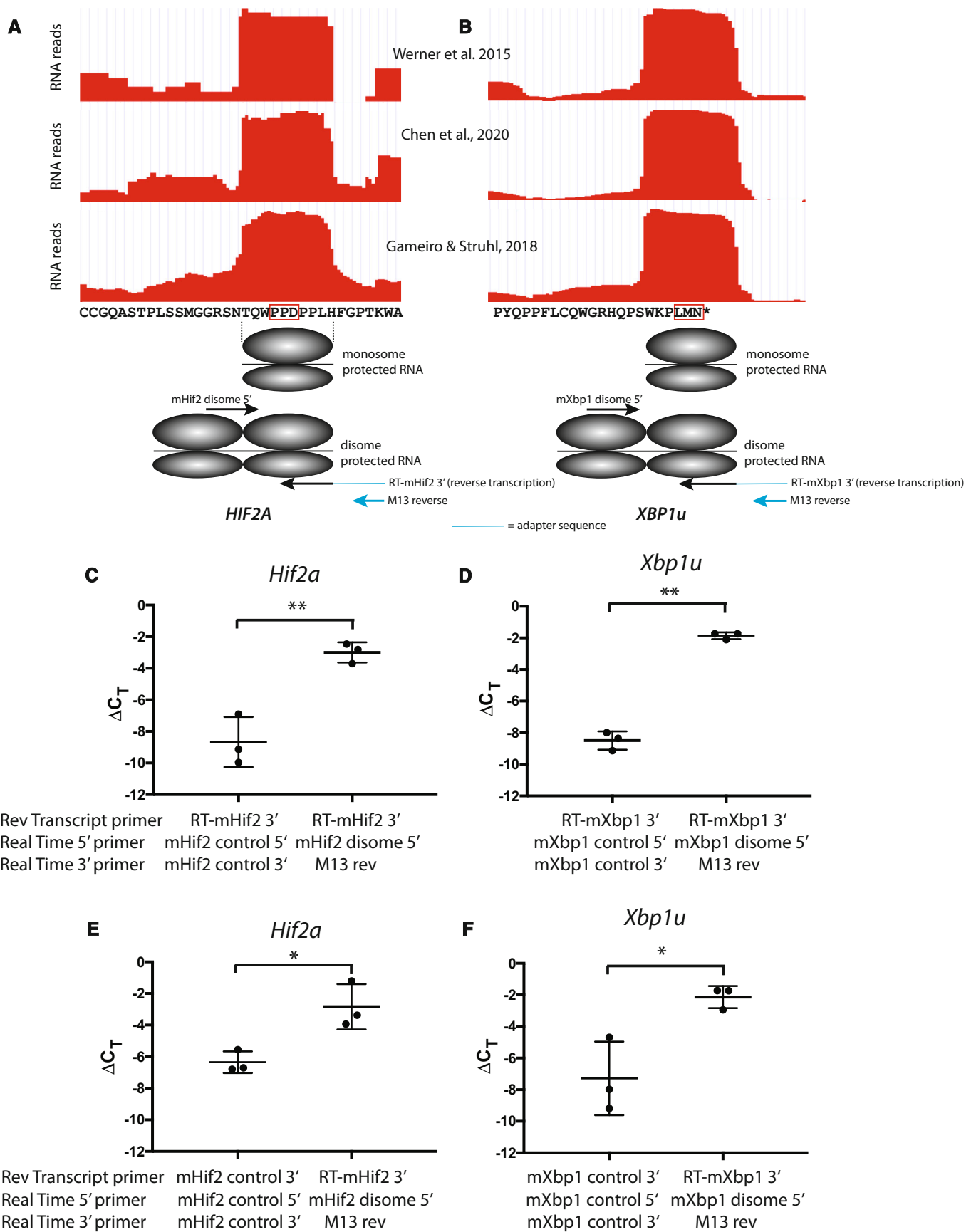


Figure 4.

Figure 4. Evidence for disome formation on the *Hif2a* mRNA.

- A, B Ribosome profiling results of sequences corresponding to the (A) proposed HIF-2 α and (B) known XBP1u translational pause sites (Werner et al, 2015; Gameiro & Struhl, 2018; Chen et al, 2020), visualized using GWIPS-viz (Michel et al, 2014). Proposed positions of monosome and disome at the pause site, and positions of primers for reverse transcription and real-time PCR are shown. * = Termination codon. Red boxes highlight the (A) proposed and (B) known tripeptide sequences that occupy the E-P-A sites in the ribosome.
- C–F Mouse kidney was lysed, treated with or without RNase I, and RNA was isolated. The RNA was reverse transcribed with the indicated primers for (C, E) *Hif2a* and (D, F) *Xbp1u* mRNA, and then analyzed by real-time PCR for disomes using the indicated primers. $\Delta C_T = (\Delta C_T = C_{T-RNase} - C_{T+RNase})$. Biological replicates (from three males), with mean \pm SD are shown. * $P < 0.05$, ** $P < 0.01$, by unpaired two-tailed t-test.

we find that the C42R mutation impairs the ability of the ZF to promote biotinylation of the HIF-2 α BAP substrate (Fig 5B, top panel). We now find that the other two mutations, Y41C and K55N, do so as well. Hence, erythrocytosis-associated ZF mutations lead to defective PHD2 binding to NACA and defective PHD2 function *in vitro*.

The Tibetan PHD2 zinc finger maintains binding to NACA

Tibetans have adapted to the chronic hypoxia of high altitude, and display evidence of natural selection of a *PHD2* haplotype that encodes for a D4E/C127S double amino acid substitution (Xiang et al, 2013; Lorenzo et al, 2014). Two important phenotypic features of Tibetan adaption are robust hypoxic ventilatory responses, and avoidance of the erythrocytosis that typically accompanies residence at high altitudes (Bigham & Lee, 2014). The two PHD2 residues (D4 and C127) that are mutated in Tibetans flank the ZF, and we have previously demonstrated that this results in impaired interaction of the PHD2 ZF with p23 (Song et al, 2014). This, in turn, could account for the augmented hypoxic ventilatory responses in Tibetans because both *p23^{AA/AA}* mice and mice with Tibetan *Phd2* display the same respiratory phenotype (Song et al, 2020).

That previous report did not study the interaction of Tibetan (Tib) PHD2 with NACA. To examine this, we coexpressed either WT or D4E/C127S PHD2 with NACA in HEK293FT cells, and then immunoprecipitated the NACA. In contrast to its previously observed effect on the PHD2:p23 interaction (Song et al, 2014), we find that the D4E/C127S mutation maintains the PHD2:NACA interaction (Fig 5C, top panel). We next fused the Tibetan PHD2 ZF to BirA (Fig 5D), prepared recombinant protein by *in vitro* translation, and then tested it in the *in vitro* biotinylation assay. As shown in Fig 5E (left, top panel), the Tibetan PHD2 ZF can induce biotinylation of the HIF-2 α BAP construct to levels comparable to that seen with the WT PHD2 ZF, and different from that of a C32S/C36S mutant (ZFmut) that ablates the ZF. A similar result is seen when the GFP-HA-BAP-HIF-2 α TPS fusion protein is employed as the substrate (Fig 5E, right, top panel).

We further tested the integrity of the Tibetan PHD2:NACA interaction by crossing the *Naca^{AA/AA}* mice with a mouse line bearing a knock-in of Tibetan *PHD2* exon 1 (*Phd2^{Tib}*, which contains the D4E/C127S substitution) (Song et al, 2020). This mouse line displays normal hematocrit and hemoglobin levels (Song et al, 2020). Our reasoning was that if there is a defect in the interaction of the Tibetan PHD2 ZF with p23 but not with Naca, then the red cell mass of Tibetan *Phd2* mice should retain sensitivity to disruption of the Phd2:Naca interaction induced by crossing these mice with the *Naca^{AA/AA}* mice. We find indeed that *Phd2^{Tib/Tib}*; *Naca^{AA/AA}* mice

display erythrocytosis as compared to *Phd2^{Tib/Tib}* mice (Fig 6A). We also examined the effect of the *Naca^{AA}* mutation in the context of a control mouse line bearing a knock-in of wild type human PHD2 exon 1 (*Phd2^{WT}*), and find that, as expected, these *Phd2^{WT/WT}*; *Naca^{AA/AA}* mice also display increased hematocrit and red blood cell counts as compared to *Phd2^{WT/WT}* mice (Fig 6B). These studies reinforce the notion that the Tibetan PHD2:NACA interaction is intact, because the PXLE > PXAA mutation retains the ability to induce an erythrocytosis in a Tibetan *Phd2* background. Importantly, they now provide an explanation of how a Tibetan *PHD2* loss of function allele (with respect to p23 interaction) can avoid predisposition to erythrocytosis (via maintained interaction with NACA).

Collectively, these findings indicate that the Tibetan PHD2 mutation behaves differently than the erythrocytosis-associated PHD2 ZF mutations. The latter impair interaction with NACA, impair PHD2 ZF function *in vitro*, and are associated with erythrocytosis *in vivo*, while the former maintains interaction with NACA, maintains PHD2 ZF function in the *in vitro* biotinylation assay, and is not associated with erythrocytosis *in vivo*.

Discussion

Prolyl hydroxylase domain protein 2 is a key oxygen sensor of the HIF pathway, and it has drawn considerable attention because of its central role in the control of red cell mass. Indeed, PHD2 inhibitors have been approved for use in Asia and Europe to treat anemia associated with chronic renal disease (Chen et al, 2019a, 2019b), and they are being considered for a host of other ischemic and inflammatory diseases (Rabinowitz, 2013; Chan et al, 2016). These inhibitors target the well-characterized prolyl hydroxylase domain of PHD2. In contrast, far less is known about its other domain, the N-terminal ZF. This domain is particularly intriguing because Tibetans possess PHD2 amino acid substitutions that flank the ZF and impair its interaction with the HSP90 cochaperone p23 (Xiang et al, 2013; Lorenzo et al, 2014; Song et al, 2014). Tibetans have adapted over the course of thousands of years to the chronic hypoxia of high altitude (Beall, 2014; Bigham & Lee, 2014; Simonson, 2015; Moore, 2017), and this altered interaction with p23 could account for the augmented hypoxic ventilatory responses that have been observed in Tibetans (Song et al, 2020).

Here we show that in addition to binding the PXLE motifs in p23, FKBP38, and HSP90, the ZF of PHD2 also binds to this motif in NACA and that this latter interaction plays a critical role in allowing PHD2 to maintain normal control over red cell mass (Table 1). NACA binds to NACB to form a heterodimeric NAC complex (Wiedmann et al, 1994), and it may be noted that PHD2 has been identified in immunoprecipitates of NACB (also known as BTF3) in large-

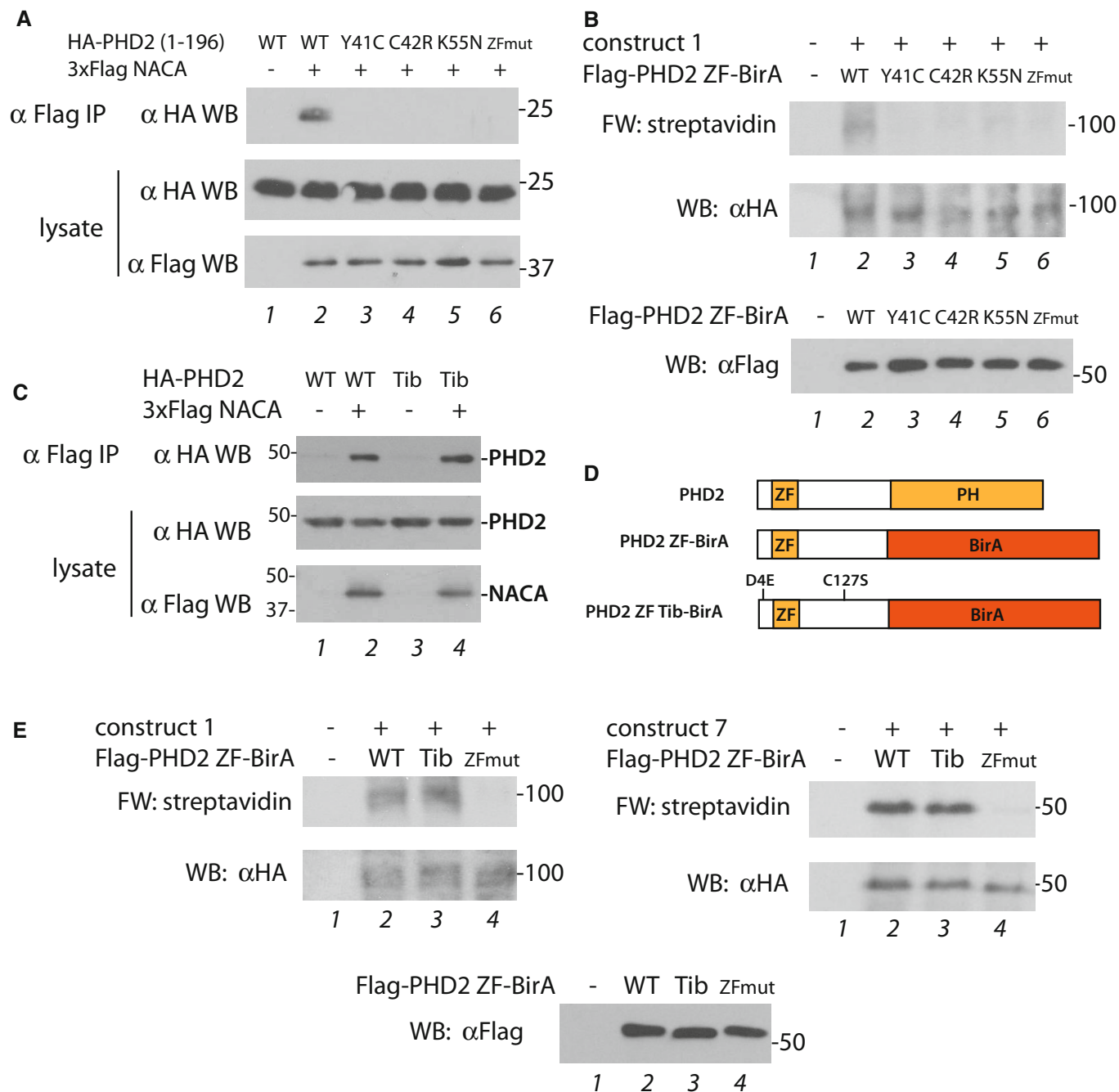


Figure 5. Erythrocytosis-associated but not Tibetan PHD2 zinc finger mutations impair binding to NACA and function.

A HEK293 FT cells were transfected with expression plasmids for the indicated proteins. The cells were lysed and subjected to immunoprecipitation with anti-Flag antibodies, and then the immunoprecipitates and aliquots of lysate were examined by western blotting as indicated. ZFmut = C36S/C42S.

B *In vitro* translation/biotinylation reactions using reticulocyte lysates and the indicated constructs. Streptavidin far western (FW) assesses biotinylation. Anti-HA western blot (WB) measures translated substrate. Bottom, the indicated proteins were prepared by *in vitro* translation using reticulocyte lysates and analyzed by α Flag western blotting.

C HEK293 FT cells were transfected with expression plasmids for the indicated proteins. Tib, Tibetan. The cells were lysed and subjected to immunoprecipitation with anti-Flag antibodies, and then the immunoprecipitates and aliquots of lysate were examined by western blotting as indicated.

D Diagram of PHD2 and constructs employed for *in vitro* translation studies. Mutations are as indicated.

E *In vitro* translation/biotinylation reactions using reticulocyte lysates and construct 1 (left) or construct 7 (right). Streptavidin far western (FW) assesses biotinylation. Anti-HA western blot (WB) measures translated substrate. Bottom, the indicated proteins were prepared by *in vitro* translation using reticulocyte lysates and analyzed by α Flag western blotting.

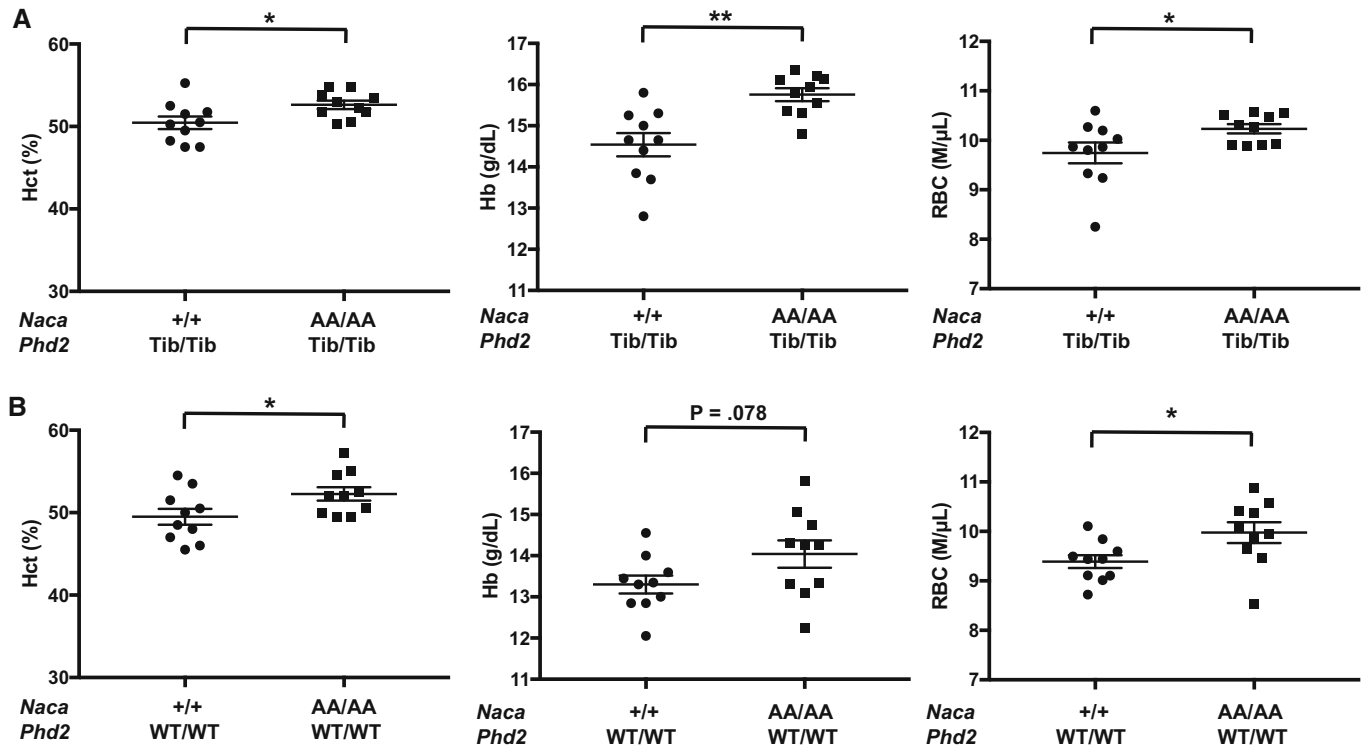


Figure 6. Naca PXLE > PXAA mutations induce erythrocytosis in Tibetan *Phd2* mice.

A, B Hct, Hb, and RBC counts were measured in (A) *Phd2*^{Tib/Tib}; *Naca*^{AA/AA} and (B) *Phd2*^{WT/WT}; *Naca*^{AA/AA} mice and compared to (A) *Phd2*^{Tib/Tib} and (B) *Phd2*^{WT/WT} controls, respectively. In (A), *n* = 10 with seven males and three females in each group. In (B), *n* = 10 with five males and five females in each group. Biological replicates, with mean ± SEM are shown. **P* < 0.05, ***P* < 0.01, by unpaired two-tailed *t*-test.

scale proteomic studies (Huttlin *et al.*, 2021). NACB lacks a PXLE motif, suggesting that this interaction is indirect and is mediated through NACA. The NAC complex is a ribosomal chaperone that plays an essential role in directing nascent polypeptides as they emerge from the ribosome exit tunnel to their proper cellular locations (Wiedmann *et al.*, 1994; Gamberdinger *et al.*, 2015). In particular, it plays an essential role in directing nascent cytosolic proteins to the cytoplasm. It competes with other complexes, particularly SRP, at the ribosome exit tunnel (Jomaa *et al.*, 2022). SRP directs proteins to the endoplasmic reticulum. The PXLE motif is strongly conserved in vertebrate NACA (Fig 1B). It is also present in NACA from some invertebrates, such as *D. melanogaster* (Appendix Table S1). Of note, it is not present in NACA from the simplest animal, *Trichoplax adhaerens*, which instead possesses p23 and HSP90 homologs that harbor PXLE motifs (Appendix Table S1).

The positioning of NACA at the port of the ribosomal exit tunnel would allow recruited PHD2 to cotranslationally prolyl hydroxylate HIF-2 α (Fig 7A). Critically, this is enhanced by a translational pause site encoded within HIF-2 α (Fig 3A). Appropriately, this pause site is C-terminal to the primary site of hydroxylation in HIF-2 α (Pro-531). If the pause site were N-terminal, it would not be expected to enhance prolyl hydroxylation, and this is borne out by the results of our *in vitro* assays evaluating the position of the pause site (Fig 3F). Furthermore, the distance between the primary site of hydroxylation (Pro-531) and pause sequence (residues 620–653) is about 100 amino acids, which would ensure the hydroxyl acceptor proline is

outside the ribosome exit tunnel (which can accommodate 30–40 amino acids) and thereby accessible for modification at the time that pausing occurs. Our model provides a mechanism by which PHD2 can efficiently scan nascent polypeptides for HIF- α substrates.

Programmed translational pauses are well described in both prokaryotes and eukaryotes (Ito & Chiba, 2013). In eukaryotes, perhaps the best-described example occurs with XBP1u, a central component of the unfolded protein response (Yanagitani *et al.*, 2011). Programmed translational pausing at the C-terminus of XBP1u allows exposure of an upstream hydrophobic polypeptide sequence that targets the *XBP1u* mRNA to the endoplasmic reticulum, where the transmembrane endoribonuclease IRE1 α splices *XBP1u* to *XBP1s*. The latter, in turn, encodes for the active transcription factor XBP1s. The translational pausing of HIF-2 α bears some similarity to that of XBP1u, but it differs in two key respects. First, instead of relying on targeting to a different cellular locale where an enzymatic activity resides, it relies on a ribosomal chaperone (NACA) that directly recruits the regulatory enzyme (PHD2). Second, instead of relying on alteration (splicing) of the mRNA to produce a distinct protein product, it involves direct cotranslational, site-specific modification (hydroxylation) of the protein. In this regard, it should also be noted that the site-specificity of this hydroxylation modification sets it apart from other cotranslational modifications that occur at the ribosome, such as modifications at the N-terminus of nascent polypeptides (Varland *et al.*, 2015). At present, it is not known whether the HIF- α translational pause is itself sensitive to oxygen

Table 1. Summary of mutations affecting the PHD2 zinc finger and its ligands, and their effects on red cell mass and ventilatory control

Gene	Organism	Mutation	Effect on red cell mass	Effect on ventilatory control	References
<i>Naca</i>	Mouse	L38A/E39A	Erythrocytosis	ND ^a	This study
<i>p23</i>	Mouse	L159A/E160A	None	Increased HVR ^b	This study and Song et al (2020)
<i>Fkbp38</i>	Mouse	L45A/E46A	None	None	This study and Song et al (2020)
Combined <i>Hsp90α</i> and <i>Hsp90β</i>	Mouse	L720A/E721A L711A/E712A	None	ND	This study
<i>Phd2</i>	Mouse	D4E/C127S	None	Increased HVR	Song et al (2020)
<i>PHD2</i>	Human	D4E/C127S	None ^c	ND	Tashi et al (2017)
<i>PHD2</i>	Human	Y41C	Erythrocytosis	ND	Sinnema et al (2018)
<i>PHD2</i>	Human	C42R	Erythrocytosis	ND	Sinnema et al (2018)
<i>PHD2</i>	Human	K55N	Erythrocytosis	ND	Song et al (2019)

^aNot determined.

^bHypoxic ventilatory response.

^cWhen examined irrespective of *EPAS1* allele status in Tibetan highlanders.

concentration or redox state, nor is it known whether disomes induced by pausing trigger either ribosome quality control or mRNA no-go decay pathways.

Prolyl hydroxylase domain protein 2 hydroxylates HIF- α at a relatively simple LXXLAP consensus sequence (Ivan et al, 2001; Jaakkola et al, 2001; Yu et al, 2001; Huang et al, 2002), raising a long-standing question of how specificity in this pathway is achieved. One factor that contributes to specificity is a peptide loop in the catalytic domain of PHD2 that is involved in substrate discrimination (Flashman et al, 2007; Villar et al, 2007). The present studies identify another factor, namely, the use of a PHD2 domain (the ZF) that allows its recruitment to the ribosome that, in turn, is coupled to and exploits a programmed translational pause. In this view, HIF- α is an efficient substrate for PHD2 because it contains both a hydroxylation motif and an appropriately positioned translational pause sequence.

There is no single strict consensus sequence for peptide sequences that induce translational pauses. Nevertheless, pausing sequences share in common the capacity to establish specific contacts within the ribosome exit tunnel. Such contacts occur in a sequence-specific manner. The HIF-2 α pause sequence that we describe here contains a WPPDPP sequence. Contained within this is a highly conserved PPD motif that is enriched at the E-P-A sites of the stalled ribosomes (Han et al, 2020). Given this, as well as assessment of previous ribosome profiling data (Fig 4A), we propose that the PPD motif occupies the E-P-A sites of the ribosome paused on the *HIF2A* mRNA. More definitive assessment of this, as well as determination of other specific contacts within the ribosome exit tunnel, must await additional studies such as structural ones. This WPPDPP sequence also contains a WPP motif. Interestingly, such a motif has been identified in a genetic selection from random libraries for sequences that can induce translational pausing in *E. coli* (Tanner et al, 2009), hinting that there may be peptide motifs that pause translation across multiple kingdoms of life.

Human erythrocytosis-associated mutations have yet to be identified in the translational pause sequence of HIF-2 α . Instead, erythrocytosis-associated mutations have been identified in both the ZF and catalytic domain of PHD2 (Lappin & Lee, 2019). At present, we have no evidence that either of these types of mutations acts by

a dominant negative mechanism. Indeed, in the case of catalytic domain mutation P317R, current evidence indicates that it acts by a haploinsufficiency mechanism (Arsenault et al, 2013).

We find that Tibetan (D4E/C127S) PHD2, while defective in its interaction with p23 (Song et al, 2014, 2020), retains its binding to NACA (Fig 5C). Consistent with this, the *Naca*^{AA} allele is able to induce erythrocytosis in a *Phd2*^{Tib/Tib} background (Fig 6A). Since NACA is the PXLE-containing protein that is critical for maintenance of normal red cell mass (Figs 1D and 7B), this now provides an explanation for why Tibetans are not predisposed to erythrocytosis despite harboring a loss of function PHD2 allele—namely, the defect selectively affects its binding to p23 but not NACA (Fig 7C). Consistent with this, it has been observed that the Tibetan *PHD2* allele (when examined irrespective of *HIF2A* allele status) is not correlated with hemoglobin levels in Tibetan highlanders (Tashi et al, 2017). Clearly, another factor that likely contributes critically to their relatively low hemoglobin levels is that they harbor a *HIF2A* allele, available evidence of which suggests to be a partial loss of function allele (Bigham & Lee, 2014). Indeed, the *HIF2A* locus is the one that is consistently most strongly correlated with hemoglobin levels in Tibetans (Beall, 2014). Our findings also distinguish the effects of the Tibetan mutation on ZF function from those associated with erythrocytosis, which disrupt interaction with NACA (Fig 7D).

Based on these current studies as well as our previously published work, we propose that the relative importance of differing PHD2 ZF: PXLE-containing protein interactions occur in an organ-specific manner (Fig 7B). In the EPO-producing cells of the kidney, the PHD2:NACA interaction plays a critical role in the normal regulation of red cell mass. In the carotid body, on the other hand, the PHD2:p23 interaction plays a critical role in the maintenance of the hypoxic ventilatory response. Whether this is due to cell-specific differences in levels of expression of the components of these pathways, posttranslational modifications, or some other mechanism remains to be determined. The cell-dependent utilization of different pathways is somewhat analogous to the manner in which transcription factors can use transcriptional coactivators in a tissue-specific manner to achieve tissue-specific gene expression (Spiegelman & Heinrich, 2004). Importantly, such an arrangement provides the template in which alterations in ZF binding properties can provide

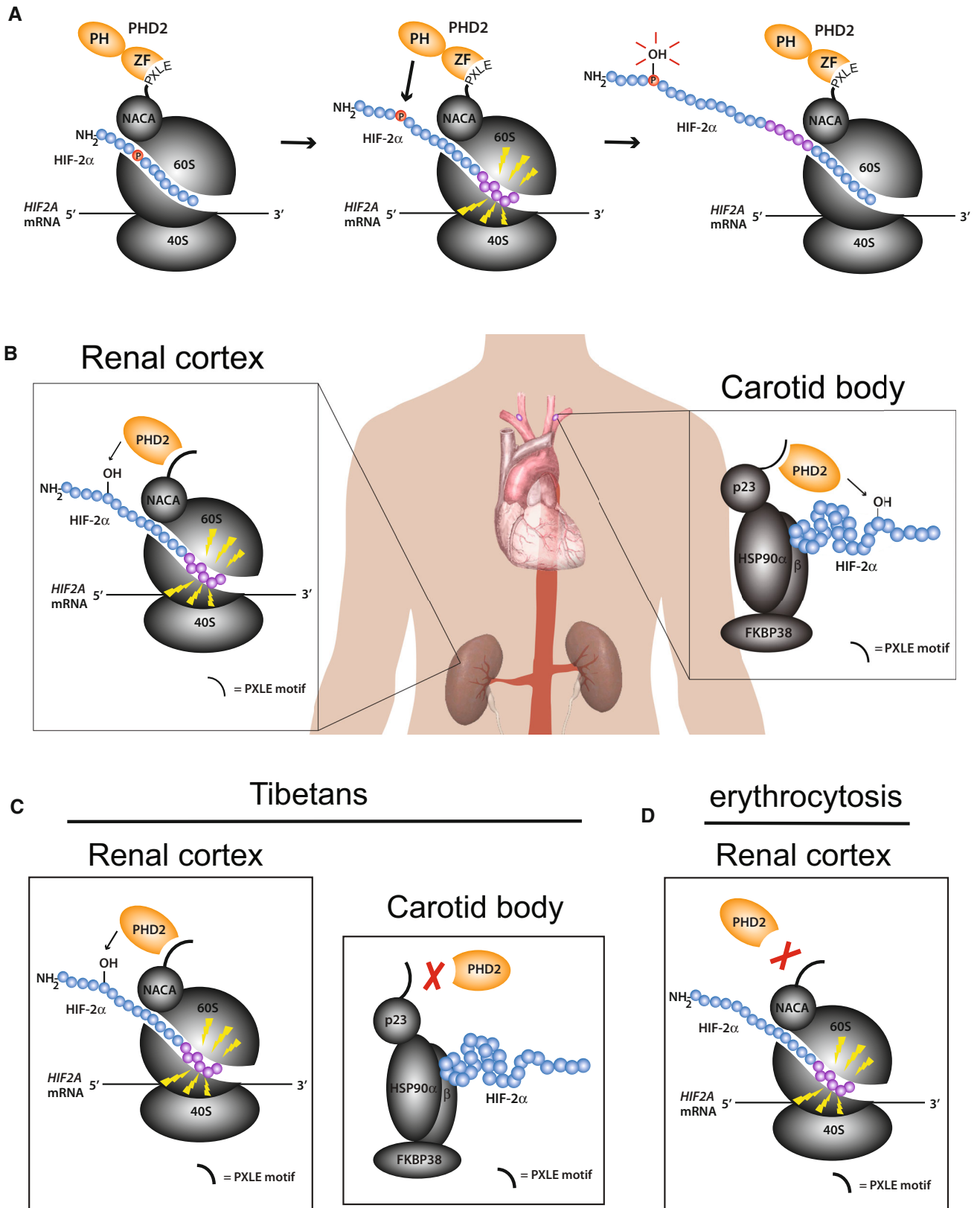


Figure 7.

Figure 7. Proposed model for PHD2 and PHD2-associated mutations.

- A Left, nascent HIF-2 α polypeptide is translated. The site of prolyl hydroxylation has not yet emerged from the ribosome exit tunnel. Middle, the translational pause sequence (purple) slows translation. PHD2, which is recruited by NACA to the ribosome exit tunnel, can then modify the exposed hydroxyl acceptor prolyl residue (red). Right, prolyl hydroxylated HIF-2 α emerges from the ribosome exit tunnel.
- B In the EPO-producing cells of the renal cortex, PHD2 is recruited to the translation machinery by NACA. In the carotid body, PHD2 is recruited to the HSP90 pathway by the HSP90 cochaperone p23.
- C Tibetan PHD2 has a selective defect in interaction with p23, but not with NACA, leading to a loss of function (LOF) phenotype in the carotid body. However, Tibetan PHD2 does not produce an LOF phenotype (erythrocytosis) in the EPO-producing cells of the renal cortex because PHD2 interaction with NACA is preserved.
- D Erythrocytosis-associated PHD2 mutations display defective interaction with NACA.

selective alterations in HIF outputs to facilitate adaptation to the chronic hypoxia of high altitude.

Materials and Methods

Mouse lines

Hsp90 β ^{L711A/E712A} (Hsp90 β ^{AA}) mice were generated using Crispr technology. A guide RNA plasmid, pUC57-sgRNA-Hsp90 β , was constructed by subcloning into the Bsa I site of pUC57-sgRNA (a gift from Dr. Xingxu Huang, Addgene plasmid # 51132) a duplex consisting of the following two oligonucleotides: 5'-TAGGATCCTCATCGCCTTCCAGAG-3' and 5'-AAACCTCTGGAAGGCGATGAGGAT-3'. A single-stranded oligodeoxynucleotide donor (Ultram grade) was synthesized by IDT and consisted of the following sequence: 5'-GTGGCTTACTTAAATCTGTGTCTTTCTTCTTAGGCATCGATGAAGATGAGGTCAGTGCAGAGGAGCCAGTGTCTGTCTTCTGATGAGATCCCACAGCTGCAGGCGATGAGGATGCCTCGCGCATGGAAGAGGTGGA TTAAGCCTCCTGGAAGAAGCCCTGCCCTCTGTATAGTATCCCCGTGGCTCCCCAGCAGCC-3'. A construct to express Cas9, pBS-SK-Cas9, has been described (Song *et al*, 2020). *Hsp90 β* gRNA was transcribed from Dra I linearized pUC57-sgRNA-Hsp90 β using a MEGAshortscript T7 kit (Ambion Cat #AM1354). Cas9 polyadenylated mRNA was transcribed from Xba I linearized pBS-SK-Cas9 using a mMACHINE T7 Ultra Transcription kit (Ambion Cat #AM1345). Both *Hsp90 β* gRNA and Cas9 mRNA were purified using a MEGAclear kit (Ambion Cat #1908). A mixture of *Hsp90 β* gRNA (50 ng/ μ l), Cas9 mRNA (100 ng/ μ l), and donor oligonucleotide (100 ng/ μ l) was injected into the cytoplasm of fertilized C57BL/6 oocytes by the University of Pennsylvania Transgenic & Chimeric Mouse Facility. From this procedure, a male mouse with homozygous knock-in of the *Hsp90 β ^{AA}* allele was obtained. Sequencing of 10 potential off-target loci, two with 2 mismatches to the gRNA sequence and eight with 3 mismatches (there were no off-target loci with 0 or 1 mismatches in the C57BL/6 genome), did not reveal any off-target effects of the gRNA. The sequences of the primers to examine potential off-target effects are provided in Appendix Table S2. The mouse was bred to a C57BL/6J female, and a mouse with a heterozygous knock-in was obtained. Breeding of heterozygous mice yielded *Hsp90 β ^{AA/AA}* mice. These mice were maintained in a C57BL/6 background.

Hsp90 α ^{L720A/E721A} (Hsp90 α ^{AA}) mice were generated using Crispr technology in an analogous manner. A guide RNA plasmid, pUC57-sgRNA-Hsp90 α , was constructed by subcloning into the Bsa I site of pUC57-sgRNA a duplex consisting of the following two oligonucleotides: 5'-TAGGAAGAAATGCCTCCCCTGGA-3' and 5'-AA

ACTCCAGGGGAGGCATTTCTT-3'. The single-stranded oligodeoxynucleotide donor consisted of the following sequence: 5'-CGGACATTAAC TGTAACATTTATTCCAAAACAAGGTATTGATGAGGATGATCCTACT GTGGATGACACCAGTGTCTGTAAGTGAAGAAATGCCTCCAGCTG CAGGAGATGACGACACATCACGCATGGAAGAAGTAGACTAAGTC ACCAGAACTATGTGTTTGCTTACCTTCATTCCTTCTGATAATATAT TTTCCA-3'. Following injections of a mixture of the *Hsp90 α* gRNA, Cas9 mRNA, and donor oligonucleotide into fertilized C57BL/6 oocytes, a male mouse with homozygous knock-in of the *Hsp90 α ^{AA}* allele was obtained. Sequencing of two *Hsp90 α* pseudogenes with 0 mismatches to the gRNA sequence, *Hsp86-ps1*, and *Hsp86-ps2* (Moore *et al*, 1991), revealed either knock-in or deletions at these pseudogenes. Sequencing of eight additional potential off-target loci, two with 2 mismatches to the gRNA sequence and six with 3 mismatches (there were no off-target loci with 1 mismatch) did not reveal any other off-target effects of the gRNA. The sequences of the primers to examine potential off-target effects are provided in Appendix Table S3. The mouse was bred to a C57BL/6J female, and a mouse with a heterozygous knock-in was obtained. Breeding of heterozygous mice yielded *Hsp90 α ^{AA/AA}* mice. These mice were maintained in a C57BL/6 background.

Naca^{L38A/E39A} (Naca^{AA}) mice were generated using Crispr technology. A guide RNA plasmid, pUC57-sgRNA-Naca, was constructed by subcloning into the Bsa I site of pUC57-sgRNA a duplex consisting of the following two oligonucleotides: 5'-TAGGAGTCTTGTTCTCGAGCTC-3' and 5'-AAACGAGCTCGAGGAACAAGACT-3'. The single-stranded oligodeoxynucleotide donor consisted of the following sequence: 5'-TGATGAGGTGCCACCTCTTAAATTCTATTGTTGAGTAAAAGTTACCTGTCTCCTAGGATCGGGAACAGAGTCTGACAGTGTGAGTACAGTACCAGAAGCTGCAGAACAAGACTCCACACAGACGGCCACGCAGCAAGCCAGGTGTGTCTCTTAAATTAATTACTTACATTGAGTCAAGAATGCACTAGGGGACAAGTG-3'. Following injections of a mixture of the *Naca* gRNA, Cas9 mRNA, and donor oligonucleotide into fertilized C57BL/6 oocytes, a male mouse with homozygous knock-in of the *Naca^{AA}* allele was obtained. Sequencing of a single *Naca* pseudogene with 0 mismatches to the gRNA sequence revealed knock-in at this pseudogene. Sequencing of six additional potential off-target loci, two with 1 mismatch to the gRNA sequence, one with 2 mismatches, and three with 3 mismatches did not reveal any other off-target effects of the gRNA. The sequences of the primers to examine potential off-target effects are provided in Appendix Table S4. The mouse was bred to a C57BL/6J female, and a mouse with a heterozygous knock-in was obtained. In subsequent breeding, the knock-in in the pseudogene was segregated from the knock-in at the *Naca* locus. Breeding of heterozygous mice yielded *Naca^{AA/AA}* mice. These mice were maintained in a C57BL/6 background.

$p23^{L159A/E160A}$; $Naca^{\Delta38-39}$ ($p23^{AA}$; $Naca^{\Delta}$) mice were generated as follows. A mixture of *Cas9* mRNA along with *Naca* gRNA and *Naca* donor oligonucleotide prepared as above was injected into the cytoplasm of fertilized $p23^{AA/+}$ (C57BL/6 background) oocytes. From this procedure, a female mouse was obtained that was heterozygous for $p23^{AA}$ at the *p23* locus and homozygous for a 6 bp in-frame deletion at the *Naca* locus ($Naca^{\Delta}$). This deletion removes amino acids 38 and 39 from the *Naca* protein. The mouse was bred to a C57BL/6 male, and a female mouse that was heterozygous for $p23^{AA}$ at the *p23* locus and heterozygous for $Naca^{\Delta}$ was obtained. Sequencing of a single *Naca* pseudogene with 0 mismatches to the gRNA sequence revealed a 3 bp deletion at this pseudogene. Sequencing of six additional potential off-target loci, two with 1 mismatch to the gRNA sequence, one with 2 mismatches, and three with 3 mismatches revealed an off-target 1 bp insertion at one of the sites with 1 mismatch (chr4:52821593). The other five sites did not show off-target effects. The sequences of the primers to examine potential off-target effects are the same as those employed previously and are provided in Appendix Table S4. In subsequent breeding, the two alleles with off-target deletion/insertion as described above were segregated from the $p23^{AA}$; $Naca^{\Delta}$ allele. These mice were maintained in a heterozygous state in a C57BL/6 background. They were also separately backcrossed five times to 129S1/SvImJ mice (The Jackson Laboratory Stock Number 002448). The mice in these two different backgrounds were then crossed to generate $p23^{AA/AA}$; $Naca^{\Delta/\Delta}$ mice and littermate $p23^{+/+}$; $Naca^{+/+}$ controls in a mixed B6/129 background.

The $p23^{AA}$ (L159A/E160A), $Fkbp38^{AA}$ (L45A/E46A), $Phd2^{WT}$ (containing a knock-in of wild-type human *PHD2* exon 1), and $Phd2^{Tib}$ mouse lines have been previously described (Song et al, 2020). Alternate names for the genes examined in the present study are provided in Appendix Table S5.

Mice were maintained on a 12/12 h light/dark cycle and had access to standard chow and autoclaved water *ad libitum*. Unless otherwise noted, mice were examined at 2–3 months of age, with approximately equal numbers of males and females. C57BL/6J mice were obtained from The Jackson Laboratory (Stock Number 000664). All mice used in this study were on a C57BL/6J background, except for the $p23^{AA/AA}$ and the $p23^{AA/AA}$; $Naca^{\Delta/\Delta}$ mice, which were in a mixed B6/129 background. All animal procedures were approved by the Institutional Animal Care and Use Committee at the University of Pennsylvania, in compliance with Animal Welfare Assurance, under Protocols 805020 and 805519.

In vitro translation reactions

In vitro translation reactions using reticulocyte lysates were performed using TnT T7 Quick Coupled kits (Promega Cat #L1170). Typical reactions contained 0.1 μ g of template (in pcDNA3 vector), 5 μ M biotin, 1 μ M ZnCl₂, TnT T7 Quick Master Mix, and 1 μ l of *in vitro* translated FlagPHD2 (1-196)-BirA fusion protein (prepared using the same kit supplemented with 1 μ M ZnCl₂) in a total volume of 9 μ l. Reactions were carried out at 25°C for 30 min.

In vitro translation reactions using HeLa cell lysates were performed using 1-Step Human Coupled IVT kits (Thermo Fisher Cat #88882). Typical reactions contained 0.1 μ g of template (in pT7CFE1 vector), 5 μ M biotin, 1 μ M ZnCl₂, kit components, and 0.2 μ l of *in vitro* translated FlagPHD2 (1–196)-BirA fusion protein

(prepared using the same 1-Step Human Coupled IVT kit supplemented with 1 μ M ZnCl₂) in a total volume of 9 μ l. Reactions were carried out at 25°C for 30 min.

Real-time PCR assays for disomes

Assays for the presence of site-specific disome footprints were conducted by measuring RNA fragments protected from RNase I digestion essentially by the method of Li et al (2019). In brief, mouse tissue lysates were prepared, digested with RNase I, and RNA was isolated and then reverse transcribed using a primer targeting the predicted 3' end of the disome with an adapter containing the M13 reverse sequence. The cDNA fragments were quantitated by real-time PCR using a primer targeting the 5' disome and an M13 reverse primer. Several controls were performed. In one, RNase I was omitted. In a second, the cDNA fragments were amplified with primers targeting a nonspecific region upstream of the predicted disome site. In a third, the RNA was reverse transcribed using the 3' primer targeting the nonspecific upstream region, and the cDNA fragments were quantified by real-time PCR using primers targeting this nonspecific upstream region. Primer sequences are provided in Appendix Table S6.

Statistical analysis

Prism 7 software (GraphPad Software) was used for statistical analysis. Statistical analyses used unpaired two-tailed *t*-tests. *P*-values < 0.05 were considered significant. Unless otherwise specified, data are presented as mean \pm SEM. No statistical method was used to predetermine the sample size.

Data availability

All data needed to evaluate the conclusions in the article are present in the manuscript and Supplementary Materials. The study includes no data deposited in external repositories.

Expanded View for this article is available online.

Acknowledgements

We thank Dr. Jean Richa of the University of Pennsylvania Perelman School of Medicine Transgenic and Chimeric Mouse Facility for injecting Crispr reagents into oocytes to generate the $Naca^{AA}$, $Hsp90\alpha^{AA}$, $Hsp90\beta^{AA}$, and $Naca^{\Delta}$; $p23^{AA}$ mice. This facility is supported by the Institute for Diabetes, Obesity, and Metabolism; the Center for Molecular Studies in Digestive and Liver Diseases; and the Abramson Cancer Center. We thank Dr. Xingxu Huang for the gift of the pUC57-sgRNA plasmid. This work was supported by NIH grants R01-HL159611 and R33-HL120751 (to FSL).

Author contributions

Daisheng Song: Conceptualization; investigation; writing – original draft. **Kai**

Peng: Conceptualization; investigation; writing – review and editing.

Bradleigh E Palmer: Investigation; writing – review and editing. **Frank S Lee:** Conceptualization; funding acquisition; investigation; writing – original draft.

Disclosure and competing interests statement

The authors declare that they have no conflict of interest.

References

- Ali MM, Roe SM, Vaughan CK, Meyer P, Panaretou B, Piper PW, Prodromou C, Pearl LH (2006) Crystal structure of an Hsp90-nucleotide-p23/Sba1 closed chaperone complex. *Nature* 440: 1013–1017
- Arsenault PR, Pei F, Lee R, Kerestes H, Percy MJ, Keith B, Simon MC, Lappin TR, Khurana TS, Lee FS (2013) A Knock-in mouse model of human PHD2 gene-associated erythrocytosis establishes a haploinsufficiency mechanism. *J Biol Chem* 288: 33571–33584
- Arsenault PR, Song D, Chung YJ, Khurana TS, Lee FS (2016) The zinc finger of prolyl hydroxylase domain protein 2 is essential for efficient hydroxylation of hypoxia-inducible factor alpha. *Mol Cell Biol* 36: 2328–2343
- Beall CM (2014) Adaptation to high altitude: phenotypes and genotypes. *Ann Rev Anthropol* 43: 251–272
- Bigham AW, Lee FS (2014) Human high-altitude adaptation: forward genetics meets the HIF pathway. *Genes Dev* 28: 2189–2204
- Bruick RK, McKnight SL (2001) A conserved family of prolyl-4-hydroxylases that modify HIF. *Science* 294: 1337–1340
- Bulgakov OV, Eggenschwiler JT, Hong DH, Anderson KV, Li T (2004) FKBP8 is a negative regulator of mouse sonic hedgehog signaling in neural tissues. *Development* 131: 2149–2159
- Chan MC, Holt-Martyn JP, Schofield CJ, Ratcliffe PJ (2016) Pharmacological targeting of the HIF hydroxylases – a new field in medicine development. *Mol Aspects Med* 47–48: 54–75
- Chen N, Hao C, Liu BC, Lin H, Wang C, Xing C, Liang X, Jiang G, Liu Z, Li X et al (2019a) Roxadustat treatment for anemia in patients undergoing long-term dialysis. *N Engl J Med* 381: 1011–1022
- Chen N, Hao C, Peng X, Lin H, Yin A, Hao L, Tao Y, Liang X, Liu Z, Xing C et al (2019b) Roxadustat for anemia in patients with kidney disease not receiving dialysis. *N Engl J Med* 381: 1001–1010
- Chen J, Brunner AD, Cogan JZ, Nunez JK, Fields AP, Adamson B, Itzhak DN, Li JY, Mann M, Leonetti MD et al (2020) Pervasive functional translation of noncanonical human open reading frames. *Science* 367: 1140–1146
- Deuerling E, Gamerding M, Kreft SG (2019) Chaperone interactions at the ribosome. *Cold Spring Harb Perspect Biol* 11: a033977
- Edgar RC (2004) MUSCLE: multiple sequence alignment with high accuracy and high throughput. *Nucleic Acids Res* 32: 1792–1797
- Epstein AC, Gleadle JM, McNeill LA, Hewitson KS, O'Rourke J, Mole DR, Mukherji M, Metzger E, Wilson MI, Dhanda A et al (2001) *C. elegans* EGL-9 and mammalian homologs define a family of dioxygenases that regulate HIF by prolyl hydroxylation. *Cell* 107: 43–54
- Flashman E, Bagg EA, Chowdhury R, Mecnovic J, Loenarz C, McDonough MA, Hewitson KS, Schofield CJ (2007) Kinetic rationale for selectivity towards N- and C-terminal oxygen dependent degradation domain substrates mediated by a loop region of HIF prolyl hydroxylases. *J Biol Chem* 283: 3808–3815
- Gameiro PA, Struhl K (2018) Nutrient deprivation elicits a transcriptional and translational inflammatory response coupled to decreased protein synthesis. *Cell Rep* 24: 1415–1424
- Gamerding M, Hanebuth MA, Frickey T, Deuerling E (2015) The principle of antagonism ensures protein targeting specificity at the endoplasmic reticulum. *Science* 348: 201–207
- Gamerding M, Kobayashi K, Wallisch A, Kreft SG, Sailer C, Schlomer R, Sachs N, Jomaa A, Stengel F, Ban N et al (2019) Early scanning of nascent polypeptides inside the ribosomal tunnel by NAC. *Mol Cell* 75: 996–1006
- Gardie B, Percy MJ, Hoogewijs D, Chowdhury R, Bento C, Arsenault PR, Richard S, Almeida H, Ewing J, Lambert F et al (2014) The role of PHD2 mutations in the pathogenesis of erythrocytosis. *Hypoxia (Auckl)* 2: 71–90
- Grad I, McKee TA, Ludwig SM, Hoyle GW, Ruiz P, Wurst W, Floss T, Miller CA 3rd, Picard D (2006) The Hsp90 cochaperone p23 is essential for perinatal survival. *Mol Cell Biol* 26: 8976–8983
- Grad I, Cederroth CR, Walicki J, Grey C, Barluenga S, Winssinger N, De Massy B, Nef S, Picard D (2010) The molecular chaperone Hsp90 alpha is required for meiotic progression of spermatocytes beyond pachytene in the mouse. *PLoS One* 5: e15770
- Han P, Shichino Y, Schneider-Poetsch T, Mito M, Hashimoto S, Udagawa T, Kohno K, Yoshida M, Mishima Y, Inada T et al (2020) Genome-wide survey of ribosome collision. *Cell Rep* 31: 107610
- Hekmatnejad B, Mandic V, Yu VW, Akhouayri O, Arabian A, St-Arnaud R (2014) Altered gene dosage confirms the genetic interaction between FIAT and alphaNAC. *Gene* 538: 328–333
- Huang J, Zhao Q, Mooney SM, Lee FS (2002) Sequence determinants in hypoxia-inducible factor-1alpha for hydroxylation by the prolyl hydroxylases PHD1, PHD2, and PHD3. *J Biol Chem* 277: 39792–39800
- Huttlin EL, Bruckner RJ, Navarrete-Perea J, Cannon JR, Baltier K, Gebreab F, Gygi MP, Thornock A, Zarraga G, Tam S et al (2021) Dual proteome-scale networks reveal cell-specific remodeling of the human interactome. *Cell* 184: 3022–3040
- Ito K, Chiba S (2013) Arrest peptides: cis-acting modulators of translation. *Annu Rev Biochem* 82: 171–202
- Ivan M, Kondo K, Yang H, Kim W, Valiando J, Ohh M, Salic A, Asara JM, Lane WS, Kaelin WG Jr (2001) HIF1alpha targeted for VHL-mediated destruction by proline hydroxylation: implications for O2 sensing. *Science* 292: 464–468
- Ivan M, Haberberger T, Gervasi DC, Michelson KS, Gunzler V, Kondo K, Yang H, Sorokina I, Conaway RC, Conaway JW et al (2002) Biochemical purification and pharmacological inhibition of a mammalian prolyl hydroxylase acting on hypoxia-inducible factor. *Proc Natl Acad Sci USA* 99: 13459–13464
- Jaakkola P, Mole DR, Tian YM, Wilson MI, Gielbert J, Gaskell SJ, Kriegsheim AV, Hebestreit HF, Mukherji M, Schofield CJ et al (2001) Targeting of HIF-1alpha to the von Hippel-Lindau ubiquitylation complex by O2-regulated prolyl hydroxylation. *Science* 292: 468–472
- Jagus R, Beckler GS (2003) Overview of eukaryotic *in vitro* translation and expression systems. *Curr Protoc Cell Biol* Chapter 11: Unit 11.1
- Jomaa A, Gamerding M, Hsieh HH, Wallisch A, Chandrasekaran V, Ulusoy Z, Scialoi A, Hegde RS, Shan SO, Ban N et al (2022) Mechanism of signal sequence handover from NAC to SRP on ribosomes during ER-protein targeting. *Science* 375: 839–844
- Kaelin WG Jr, Ratcliffe PJ (2008) Oxygen sensing by metazoans: the central role of the HIF hydroxylase pathway. *Mol Cell* 30: 393–402
- Lappin TR, Lee FS (2019) Update on mutations in the HIF: EPO pathway and their role in erythrocytosis. *Blood Rev* 37: 100590
- Lee FS, Percy MJ (2011) The HIF pathway and erythrocytosis. *Annu Rev Pathol* 6: 165–192
- Li BB, Qian C, Roberts TM, Zhao JJ (2019) Targeted profiling of RNA translation. *Curr Protoc Mol Biol* 125: e71
- Liu Y, Hu Y, Li X, Niu L, Teng M (2010) The crystal structure of the human nascent polypeptide-associated complex domain reveals a nucleic acid-binding region on the NACA subunit. *Biochemistry* 49: 2890–2896
- Loenarz C, Coleman ML, Boleininger A, Schierwater B, Holland PW, Ratcliffe PJ, Schofield CJ (2011) The hypoxia-inducible transcription factor pathway regulates oxygen sensing in the simplest animal, *Trichoplax adhaerens*. *EMBO Rep* 12: 63–70
- Lorenzo FR, Huff C, Myllymaki M, Olenchok B, Swierczek S, Tashi T, Gordeuk V, Wuren T, Ri-Li G, McClain DA et al (2014) A genetic mechanism for Tibetan high-altitude adaptation. *Nat Genet* 46: 951–956

- Martin EM, Jackson MP, Gamberdinger M, Gense K, Karamonos TK, Humes JR, Deuerling E, Ashcroft AE, Radford SE (2018) Conformational flexibility within the nascent polypeptide-associated complex enables its interactions with structurally diverse client proteins. *J Biol Chem* 293: 8554–8568
- McGlincy NJ, Ingolia NT (2017) Transcriptome-wide measurement of translation by ribosome profiling. *Methods* 126: 112–129
- Meydan S, Guydosh NR (2021) A cellular handbook for collided ribosomes: surveillance pathways and collision types. *Curr Genet* 67: 19–26
- Michel AM, Fox G, M Kiran A, De Bo C, O'Connor PB, Heaphy SM, Mullan JP, Donohue CA, Higgins DG, Baranov PV (2014) GWIPS-viz: development of a ribo-seq genome browser. *Nucleic Acids Res* 42: D859–D864
- Moore LG (2017) Human genetic adaptation to high altitudes: current status and future prospects. *Quat Int* 461: 4–13
- Moore SK, Appella E, Villar CJ, Kozak CA (1991) Mapping of the mouse 86-kDa heat-shock protein expressed gene (Hsp86-1) on chromosome 12 and related genes on chromosomes 3, 4, 9, and 11. *Genomics* 10: 1019–1029
- Percy MJ, Zhao Q, Flores A, Harrison C, Lappin TR, Maxwell PH, McMullin MF, Lee FS (2006) A family with erythrocytosis establishes a role for prolyl hydroxylase domain protein 2 in oxygen homeostasis. *Proc Natl Acad Sci USA* 103: 654–659
- Rabinowitz MH (2013) Inhibition of hypoxia-inducible factor prolyl hydroxylase domain oxygen sensors: tricking the body into mounting orchestrated survival and repair responses. *J Med Chem* 56: 9369–9402
- Semenza GL (2012) Hypoxia-inducible factors in physiology and medicine. *Cell* 148: 399–408
- Shanmuganathan V, Schiller N, Magouloupoulou A, Cheng J, Braunger K, Cymer F, Berninghausen O, Beatrix B, Kohno K, von Heijne G et al (2019) Structural and mutational analysis of the ribosome-arresting human XBP1u. *Elife* 8: e46267
- Simonson TS (2015) Altitude adaptation: a glimpse through various lenses. *High Alt Med Biol* 16: 125–137
- Sinnema M, Song D, Guan W, Janssen JWH, van Wijk R, Navalsky BE, Peng K, Donker AE, Stegmann APA, Lee FS (2018) Loss-of-function zinc finger mutation in the EGLN1 gene associated with erythrocytosis. *Blood* 132: 1455–1458
- Song D, Li LS, Heaton-Johnson KJ, Arsenault PR, Master SR, Lee FS (2013) Prolyl hydroxylase domain protein 2 (PHD2) binds a pro-Xaa-leu-Glu motif, linking it to the heat shock protein 90 pathway. *J Biol Chem* 288: 9662–9674
- Song D, Li LS, Arsenault PR, Tan Q, Bigham AW, Heaton-Johnson KJ, Master SR, Lee FS (2014) Defective Tibetan PHD2 binding to p23 links high altitude adaptation to altered oxygen sensing. *J Biol Chem* 289: 14656–14665
- Song D, Guan W, Coon LM, Al-Kali A, Oliveira JL, Lee FS (2019) An erythrocytosis-associated mutation in the zinc finger of PHD2 provides insights into its binding of p23. *Hypoxia (Auckl)* 7: 81–86
- Song D, Navalsky BE, Guan W, Ingersoll C, Wang T, Loro E, Eeles L, Matchett KB, Percy MJ, Walsby-Tickle J et al (2020) Tibetan PHD2, an allele with loss-of-function properties. *Proc Natl Acad Sci USA* 117: 12230–12238
- Spiegelman BM, Heinrich R (2004) Biological control through regulated transcriptional coactivators. *Cell* 119: 157–167
- Tanner DR, Cariello DA, Woolstenhulme CJ, Broadbent MA, Buskirk AR (2009) Genetic identification of nascent peptides that induce ribosome stalling. *J Biol Chem* 284: 34809–34818
- Tashi T, Scott Reading N, Wuren T, Zhang X, Moore LG, Hu H, Tang F, Shestakova A, Lorenzo F, Burjanivova T et al (2017) Gain-of-function EGLN1 prolyl hydroxylase (PHD2 D4E:C127S) in combination with EPAS1 (HIF-2alpha) polymorphism lowers hemoglobin concentration in Tibetan highlanders. *J Mol Med (Berl)* 95: 665–670
- Varland S, Osberg C, Arnesen T (2015) N-terminal modifications of cellular proteins: the enzymes involved, their substrate specificities and biological effects. *Proteomics* 15: 2385–2401
- Villar D, Vara-Vega A, Landazuri MO, Del Peso L (2007) Identification of a region on hypoxia-inducible-factor prolyl 4-hydroxylases that determines their specificity for the oxygen degradation domains. *Biochem J* 408: 231–240
- Voss AK, Thomas T, Gruss P (2000) Mice lacking HSP90beta fail to develop a placental labyrinth. *Development* 127: 1–11
- Waterhouse AM, Procter JB, Martin DM, Clamp M, Barton GJ (2009) Jalview version 2—a multiple sequence alignment editor and analysis workbench. *Bioinformatics* 25: 1189–1191
- Werner A, Iwasaki S, McGourty CA, Medina-Ruiz S, Teerikorpi N, Fedrigo I, Ingolia NT, Rape M (2015) Cell-fate determination by ubiquitin-dependent regulation of translation. *Nature* 525: 523–527
- Wiedmann B, Sakai H, Davis TA, Wiedmann M (1994) A protein complex required for signal-sequence-specific sorting and translocation. *Nature* 370: 434–440
- Xiang K, Ouzuluobu, Peng Y, Yang Z, Zhang X, Cui C, Zhang H, Li M, Zhang Y, Bianba et al (2013) Identification of a Tibetan-specific mutation in the hypoxic gene EGLN1 and its contribution to high-altitude adaptation. *Mol Biol Evol* 30: 1889–1898
- Yanagitani K, Kimata Y, Kadokura H, Kohno K (2011) Translational pausing ensures membrane targeting and cytoplasmic splicing of XBP1u mRNA. *Science* 331: 586–589
- Yu F, White SB, Zhao Q, Lee FS (2001) HIF-1alpha binding to VHL is regulated by stimulus-sensitive proline hydroxylation. *Proc Natl Acad Sci USA* 98: 9630–9635